Published in final edited form as:

J Comp Neurol. 2023 November ; 531(16): 1651–1668. doi:10.1002/cne.25523.

Lower jaw-to-forepaw rapid and delayed reorganization in the rat forepaw barrel subfield (FBS) in primary somatosensory cortex (SI)

Violeta Pellicer-Morata[1], **Lie Wang**[2], **Amy de Jongh Curry**[3], **Jack W. Tsao**[4], **Robert S. Waters**[2,3,*]

[1]Department of Physiology, University of Tennessee Health Science Center, College of Medicine, 956 Court Avenue, Memphis, TN 38163, USA

[2]Department of Anatomy and Neurobiology, University of Tennessee Health Science Center, College of Medicine, 855 Monroe Avenue, Suite, Memphis, TN 38163, USA

[3]Department of Biomedical Engineering, University of Memphis, Herff College of Engineering, 3815 Central Avenue, Memphis, TN 38152, USA

[4]Department of Neurology, New York University, Langone School of Medicine, 550 1st Avenue, New York, NY 10016, USA

Abstract

We used the forepaw barrel subfield (FBS) in rat primary somatosensory cortex in adult rats as a model system to study rapid and delayed lower jaw-to-forepaw cortical reorganization. Multi-unit recording from FBS neurons was used to examine peripheral input to the FBS, that normally receive somatotopic input from the forepaw skin surface, for the presence of lower jaw input following deafferentations that include forelimb amputation, brachial plexus nerve cut, and brachial plexus anesthesia. The major findings are: 1) immediately following forelimb deafferentations, new input from the lower jaw becomes expressed in the anterior FBS; (2) seven-to-27 weeks after forelimb amputation, new input from the lower jaw is expressed in both anterior and posterior FBS; (3) evoked response latencies recorded in the deafferented FBS following electrical stimulation of the lower jaw skin surface are significantly longer in both rapid and delayed deafferents compared to control latencies for input from the forepaw to reach the FBS or for input from lower jaw to reach the LJBSF; (4) the longer latencies suggests that an additional relay site is imposed along the somatosensory pathway for lower jaw input to access the deafferented FBS. We conclude that different sources of input and different mechanisms underlie

*Corresponding author at: Department of Anatomy and Neurobiology, University of Tennessee Health Science Center, College of Medicine, 855 Monroe Avenue, Memphis, TN 38163, USA, rwaters@uthsc.edu.

Lie Wang and Violeta Pellicer-Morata are co-first authors

Author Contributions

Violeta Pellicer-Morata: Investigation, Writing – original draft.

Lie Wang: Investigation, Methodology, Data Analyses, Supervision

Amy de Jongh Curry: Investigation

Jack W. Tsao: Writing, Funding acquisition

Robert S. Waters: Conceptualization, Investigation, Methodology, Writing - Review and Editing, Supervision, Funding acquisition.

Conflict of Interest

The authors declare no competing financial interest.

rapid and delayed reorganization in the FBS and suggest that these findings are relevant, as an initial step, for developing a rodent animal model to investigate phantom limb phenomena.

Graphical Abstract

The rat forepaw is precisely represented in the forepaw barrel subfield (FBS) of the somatosensory cortex. Following loss of input to the forelimb, the anterior FBS begins responding to stimulation of the lower jaw. Seven weeks later, the entire FBS becomes responsive. Different sources and mechanisms underlie rapid and delayed reorganization and are explored in this rodent animal model.

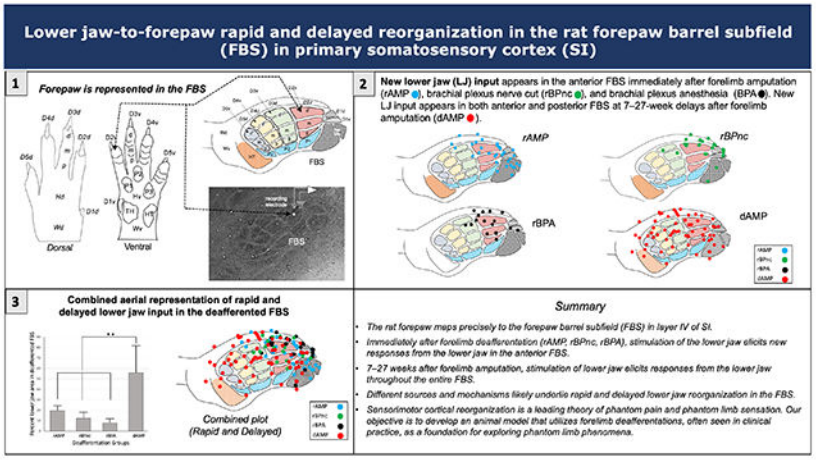

Keywords

cortical reorganization; hand-to-face remapping; barrel cortex; brain mapping; somatosensory cortex; sensorimotor cortex; rodent barrel field; forepaw barrel subfield; FBS; phantom pain

INTRODUCTION

The forelimb representation in layer IV of primary somatosensory cortex (SI) receives somatotopically organized input from the contralateral forelimb. When this input is prevented by peripheral or central disruption of afferents, cells in the deafferented forelimb SI become responsive to new input from a neighboring body surface, a condition described as cortical representational reorganization. Long and short-term disruption of somatosensory afferents following amputation or nerve cut lead to delayed and rapid cortical reorganization very likely served by different underlying mechanisms (Calford 2002).

Delayed cortical reorganization –

In an early study, Kalaska and Pomeranz cut the forelimb nerves innervating the cat forepaw cortex and reported that 6–8 weeks later, cells in the deafferented forepaw cortex responded to new input from the adjacent forearm (Kalaska and Pomeranz 1979). Delayed cortical reorganization following forelimb nerve cut or amputation was subsequently reported in monkey (Merzenich, Kaas et al. 1983a, Merzenich, Kaas et al. 1983b, Garraghty and Kaas 1991), cat (Kalaska and Pomeranz 1979, McKinley, Jenkins et al. 1987, Dykes, Avendano et

al. 1995), flying fox (Calford and Tweedale 1988), raccoon (Rasmusson 1982, Rasmusson, Turnbull et al. 1985), and rat (McCandlish, Li et al. 1996, Pearson, Li et al. 1999). These reorganization findings were extended when investigators reported that 12 years after monkeys underwent a dorsal rhizotomy, new input from the face and lower jaw moved into the deafferented forelimb SI (Pons, Garraghty et al. 1991); while the face and lower jaw are non-adjacent body part skin regions, their representations in SI lie adjacent to one another in SI (Kaas, Nelson et al. 1979, Pons, Wall et al. 1987). Subsequently, other investigators reported new face and lower jaw input in deprived SI in monkeys examined six or more months after deafferentation (Jain, Catania et al. 1997, Jain, Florence et al. 2000, Jain, Qi et al. 2008).

Rapid cortical reorganization –

Studies in monkey where SI remapping takes place immediately following median nerve transection (Merzenich, Kaas et al. 1983a), digit amputation or local injection of lidocaine (Calford and Tweedale 1991), and in flying fox (bat) immediately following digit amputation (Calford and Tweedale 1988, Calford and Tweedale 1991) reveal a greatly expanded representation of adjacent digits. Similarly in rat, where local anesthesia applied to selected vibrissae in the whisker pad and gum result in immediate response of adjacent facial whiskers in SI as well as immediate unmasking in subcortical nuclei in thalamus and brainstem (Faggin, Nguyen et al. 1997), and 1-to-2-days after severing the sciatic nerve in adult rats, investigators reported new input from the saphenous nerve expanded into the deafferented hindpaw SI (Wall and Cusick 1984).

While rapid reorganization is reported in monkey and bat following digit deafferentation, no studies that we are aware, examined rapid hand-to-lower jaw reorganization following forelimb deafferentation. However, several research groups found new lower jaw input in the deafferented forepaw representation in the forepaw barrel subfield (FBS) in SI following forelimb amputation or forelimb nerve transection in adult rats (Hickmott and Merzenich 2002, Pluto, Lane et al. 2003, Oliveira, Bittencourt-Navarrete et al. 2014). In an early study, two or more months after a mid-humerus forelimb amputation in adult rats, investigators reported a small percentage of sites in the deafferented FBS responded to new input from the face however the majority of sites in the deafferented FBS responded to input from the stump (Pluto, Lane et al. 2003). In a later study on forelimb nerve regeneration, investigators observed that immediately following transection of the radial, ulnar, and median nerve branches at the level of the brachial plexus, sparse input from the lower jaw appeared along the anterior border of the deafferented FBS (Oliveira, Bittencourt-Navarrete et al. 2014). In another study that examined the circuit properties at the border between the lower jaw barrel subfield (LJBSF) and adjacent FBS in adult rats that underwent transection of ulnar, radial, and median nerves, investigators found both rapid and delayed shifts in the location of the border into the deafferented FBS (Hickmott and Merzenich 2002).

Rodents offer important animal models for studying cortical forelimb development (McCandlish, Waters et al. 1989, Waters, McCandlish et al. 1990, McCandlish, Li et al. 1993), cortical forelimb organization (Waters, Li et al. 1995, Pearson, Oladehin et al. 1996, Pellicer-Morata, Wang et al. 2021), and cortical forelimb reorganization (Pearson,

Li et al. 1999) because of the presence of clusters of cells in layer IV of SI, called barrels, that are associated with the representation of forepaw and wrist skin surfaces. Barrels develop differentially along a lateral to medial gradient (McCandlish, Waters et al. 1989, McCandlish, Li et al. 1993) and require an intact periphery during the first seven post-natal-days (PND) for normal limb barrels to consolidate (Waters, McCandlish et al. 1990). After PND-7, forelimb deafferentation does not substantially alter the morphological organization of the forepaw barrel map, thus providing an invariant morphological map of the former limb representation in its absence. The forepaw barrel subfield (FBS) consists of approximately 25 barrels, each associated with the somatotopic representation of a discrete region on the glabrous and hairy forepaw skin surfaces that include digits, digit and palmar pads, dorsal and ventral wrist (Waters, Li et al. 1995).

In the present study, we took advantage of the invariant anatomical nature of the barrel field in adult rats to examine lower jaw-to-forepaw remapping following forelimb deafferentation that included brachial plexus nerve cut, brachial plexus anesthesia, and forelimb amputation studied immediately after amputation and at weeks-to-months later. We used flattened and tangentially cut tissue sections, stained with cytochrome oxidase (CO) in each deafferent group, to chart the locations of the newly expressed lower jaw input in the deafferented FBS, measured the aerial sizes of the new input, and measured evoked response latencies for the new input to reach the deafferented FBS. Using these measures, we observed lower jaw-to-forepaw remapping in all rapid and delayed experimental groups, we identified site-specific locations in the FBS for the newly expressed lower jaw input that significantly differed between rapid and delayed forelimb deafferentation groups, we reported significantly longer averaged evoked response latencies for the new lower jaw input to reach the deafferented SI compared to the latency for input from the forepaw to reach the intact FBS or the latency for input from the lower jaw to reach the LJBSF in forelimb intact controls, and we speculated on the possible source(s) of the newly expressed lower jaw input in the deafferented FBS.

When the face/lower jaw is stroked in a human amputee, patients often report a sensation and/or pain in the missing phantom limb, referred to as phantom limb sensation (PLS) or phantom limb pain (PLP), respectively (Ramachandran, Stewart et al. 1992). One posited theory for phantom limb phenomenon is attributed to cortical remapping, wherein the brain reorganizes somatosensory maps in response to the loss of a limb (Collins, Russell et al. 2018). Neuromagnetic imaging in SI in human forelimb amputees confirms that input from the lower jaw moves into the former hand representation in SI (Elbert, Flor et al. 1994, Yang, Gallen et al. 1994a, Yang, Gallen et al. 1994b, Flor, Elbert et al. 1995) and the extent of the lower jaw reorganization in the deafferented hand representation correlates with the magnitude of PLP experienced by the amputee (Flor, Elbert et al. 1995). Phantom limb phenomena links to maladaptive cortical plasticity which is currently a prominent theory of PLP (Collins, Russell et al. 2018). The purpose of this study was to develop a rodent animal model to investigate and compare rapid and delayed lower jaw-to-forepaw reorganization in FBS in primary somatosensory cortex (SI) using deafferentations seen in clinical practice as a starting point to investigate phantom limb phenomena.

2 | EXPERIMENTAL PROCEDURES

2.1. | Animals

Experiments were carried out on female Sprague-Dawley rats with an average body weight of 236.77 g (± 21.24 g). Experiments conformed to the *Guide for Care and Use of Laboratory Animals, Eighth Edition* and were approved by the Institutional Animal Care and Use Committee (IACUC) of the University of Tennessee Health Science Center.

2.2. | Animal preparation – forelimb deafferentation

We examined responses in the FBS in adult rats that underwent forelimb deafferentation (forelimb amputation, brachial plexus nerve cut, brachial plexus anesthesia) as described below.

rapid Forelimb Amputation (rAMP): Under aseptic conditions, rats were weighed and anesthetized with ketamine/xylazine (83/17 mg/kg, i.p.) and supplemented (10% of initial dose, i.p.) hourly throughout the surgery to maintain areflexia. Rats were placed in a supine position on a water-circulating heating pad to maintain a body temperature between 36.5–38.0°C. We monitored heart rate, breath rate, and arterial oxygen saturation (SpO_2) with a pulse oximeter (Starr Life Sciences MouseOx Plus [RRID:SCR_022984]). The hair on the upper arm and adjacent skin regions was removed with a depilatory cream. The upper arm skin was infiltrated with Marcaine (0.25% Marcaine with epinephrine, SQ). An incision was made in the skin around the humerus, and the underlying muscles were reflected to expose the brachial plexus. Brachial plexus nerves and brachial artery were ligated with fine suture (5-0 silk), isolated by lifting the suture, sectioned with fine scissors, and the limb was amputated at the glenno-humeral joint. The overlying muscles were sutured and injected with Marcaine. The skin was closed with wound clips and injected with Marcaine. *rAMP* rats were then prepared immediately for physiological mapping.

delayed Forelimb Amputation (dAMP): In this group of amputee rats, physiological mapping was delayed for weeks to months after amputation and limb amputation was carried out using gas anesthesia. Under aseptic conditions, *dAMP* rats were weighed and placed in an induction chamber and anesthetized with isoflurane 5.0% in 1.0 L 0_2. After 2 ½ min, rats were transferred to a surgical table where the head was placed in a nose cone that was infused with isoflurane 2.5% in 0.3 L 0_2. Monitoring of vital signs, injection of local anesthetic in the skin, limb removal, and suturing were identical to the above description for amputees mapped immediately after deafferentation. A systemic analgesic (Buprenorphine, 0.03 mg/kg, i.m.) and antibiotic (Penicillin G procaine 0.1cc) were administered prior to amputation. Following amputation, rats were placed in a recovery cage warmed by a heating lamp, observed until awake and ambulatory, and returned to the animal facility where they were monitored 3 × daily for the next 3 days. Rats had ad libitum access to food and water until mapping. These methods were previously described in detail (Pearson, Li et al. 1999, Pearson, Arnold et al. 2001, Li, Chappell et al. 2014).

Rapid Brachial Plexus nerve cut (rBPnc): Under aseptic conditions, rats were weighed and anesthetized with ketamine/xylazine (83/17 mg/kg, i.p.) and supplemented

(10% of initial dose, i.p.) hourly throughout the experiment to maintain areflexia. Rats were placed in a supine position on a water-circulating heating pad to maintain a body temperature between 36.5–38.0°C and a pulse oximeter placed on the hindpaw (Starr Life Sciences MouseOx Plus) was used to monitor vital signs. We applied a depilatory cream to remove the hair on the ventral axillary region and surrounding skin and infiltrated the skin with a local anesthetic (0.25% Marcaine with epinephrine, SQ). We used a scalpel to make a horizontal cut in the skin, parallel to the clavicle, to expose the pectoral muscles, which we teased apart to reveal the underlying brachial plexus nerve branches. A fine suture (5-0 silk) was inserted under each nerve branch, and the branch was lifted and sectioned with surgical scissors. The area was packed with saline-filled cotton, and the overlying skin was closed with staples. r*BPnc* rats were then prepared for physiological mapping as described below.

Rapid Brachial Plexus Anesthesia (rBPA): As described above, rats were weighed, anesthetized, monitored, and placed in a supine position. The left forelimb was extended and the hair on the subclavicular skin region was removed with depilatory cream. We used a marker pen to label a target site on the skin (0.7 cm caudal to the lateral one-third of the clavicle) for injection of anesthetic (Zhang, Cui et al. 2019). The skin was punctured with a 25-gauge needle attached to a 5-cc syringe containing 2% lidocaine. The needle was inserted to a depth of 7.0 mm, and 0.2 cc of lidocaine was slowly injected. r*BPA* rats were then prepared for physiological mapping.

2.3. | Animal preparation – physiological recording

Rats, anesthetized with ketamine/xylazine (83/17 mg/kg, i.p.), were placed in a stereotaxic apparatus. The head and neck were shaved, Marcaine was injected into the scalp, a midsagittal incision was made in the scalp, and the skin was reflected to expose the underlying bone. The cisterna magna was opened. Using Bregma as landmark, a 7-mm unilateral rectangular window was made in the skull overlying SI forelimb and lower jaw cortices. The dura was removed, and the brain surface was covered with a saline-soaked gauze to prevent drying. A recording chamber, fashioned from dental cement, was constructed around the opening and the cortical surface was bathed in silicone fluid (10,000 cs). A digital photograph of the cortical surface was taken and used to mark the surface locations of electrode penetrations in the brain.

A carbon fiber electrode, attached to a Canberra-type microdrive, was inserted in SI at a depth of 700 microns within the layer IV barrels, and used to record receptive fields of neurons (Waters, Li et al. 1995). Neuronal signals were amplified using a custom-built amplifier, fed into an audio monitor, and viewed on an oscilloscope. Signals were also sent to an A/D converter (Instrutech) and into a MAC computer where they were viewed and processed using custom programs written in IGOR Pro 6.37 (Wavemetrics, [RRID:SCR_000325]). Receptive fields were measured using mechanical stimulation applied to the skin with a hand-held probe or by brushing the skin surface with a fine-tipped brush. We made rows of electrode penetrations to map the entire FBS that were spaced approximately 500 microns apart; rows began anteriorly at the caudal LJBSF and advanced posteriorly to the hindpaw barrel subfield (HBS). Electrode penetrations within rows were spaced approximately 300 microns apart.

2.4. | Histological processing

Selected recording sites in SI were identified by making electrolytic lesions using cathodal pulses (5-μA × 10 s). At the end of the experiment, rats were administered a surgical-level dose of ketamine/xylazine (83/17 mg/kg, i.p.) and placed in an induction chamber where they were further anesthetized with Isoflurane 5.0% in 1 L 0_2 for 3 minutes. Rats were transferred to a fume-hood and transcardially perfused with 0.9% saline followed by chilled 4% paraformaldehyde in 0.15 M sodium phosphate–buffered saline (NaPBS, pH 7.4, 21°C). Brains were removed and hemispheres were separated and flattened between two glass slides in 4% paraformaldehyde and refrigerated overnight at 4°C. The following day flattened hemispheres were sectioned tangentially at 100 μm thickness using a vibratome. Sections were rinsed (3 × 10 min) with 0.01 M potassium phosphate–buffered saline (KPBS, pH 7.4, 21°C) and counterstained with cytochrome oxidase (CO) in a diaminobenzidine (DAB)-sucrose-PBS mixture and placed in a warm water (38°C) bath until barrels were visible (modified from Wong-Riley and Welt, 1980). Sections were rinsed (3 × 10 min) in buffer, mounted in distilled water on gelatin-coated glass slides, air dried overnight, and cover slipped.

2.5 | Data analyses

Reconstruction of electrode penetrations ––We plotted the surface point of entry of electrode penetrations and receptive fields recorded in these penetrations onto a digital photograph of the cortical surface. We identified penetration sites where lesions were recovered in flattened-tangentially cut 100-micron-thick sections of the barrel field. Receptive field and barrel field maps were fed into a computer and the maps were aligned using lesions as fiducial points and adjusted so that no more than a 25-micron difference existed between any associated lesion site in the two maps. Receptive fields recorded at individual penetration sites were then extrapolated from lesion sites and plotted onto the barrel field map for each rat.

FBS template ––To investigate the effects of forelimb deafferentation on changes in responsiveness of skin locations that can activate a site in the cortex, we employed a FBS template that was previously described (Waters, Li et al. 1995). A drawing of the dorsal and ventral surfaces of the forepaw is shown in Figure 1(a) and an interpretative summary of their representation in the FBS is shown in Figure 1(b). The FBS served as a template to plot receptive fields, from each deafferented group, onto a single map. To accomplish this, electrode penetrations from individual experiments were fitted onto the FBS template by adjusting FBS size and shape to match the template. In those experiments where lesion sites were recovered within specific barrels in the FBS, receptive fields were plotted directly onto the respective barrels in the FBS template.

Areal reconstruction ––Total FBS area and total area within the FBS where responses from the lower jaw were recorded following forelimb deafferentation were measured using ImageJ (NIH, 1.52a, developed by Wayne Rasband [RRID:SCR_003070]) from flattened and tangentially-cut tissue sections. Measurements for mean total FBS area and mean area of newly recorded lower jaw responses in the FBS were subjected to Mann-Whitney U non-parametric statistical test with a confidence level of $P<0.05$.

Evoked response latency measurements ——We used a bipolar stimulating electrode, constructed from a pair of twisted silver wires (0.75 mm tip separation) to deliver single constant-current cathodal pulses (1.5 × threshold, 1 ms pulse duration, 1 Hz frequency) to the skin surface to examine evoked response latencies in the intact and deafferented FBS. Evoked response latencies were also examined in the LJBSF following stimulation of the lower jaw. Averaged evoked response latencies were collected from 25 consecutive stimulations using customized data acquisition and analysis programs written in IGOR Pro 6.37 (Wavemetrics). Latency measures were subjected to the Mann Whitney U non-parametric statistic with a confidence level of $P<0.05$. Raster plots and post-stimulus-time histograms (PSTH) were generated in IGOR using a software toolkit (NeuroMatic [RRID:SCR 004186], Rothman and Silver 2018). A voltage spike threshold was set during the first 10 ms of baseline recording, and the same threshold was used for all measures taken at individual recording sites throughout the experiment. Spike-rasters and histograms were generated in 2-ms time bins.

3 | RESULTS

3.1. | Lower jaw-to forepaw remapping following forelimb deafferentation

Three types of forelimb deafferentations were used that included forelimb amputation (AMP), brachial plexus nerve cut (BPnc), and brachial plexus anesthesia (BPA). In one rat group, designated rapid group (rAMP, rBPnc, rBPA), rats underwent one type of deafferentation and the FBS was mapped approximately 30 min after deafferentation. In the initial two experiments in each rapid deafferentation group, pre-deafferentation mapping of FBS provided evidence that only forepaw responses were recorded in the FBS; pre-deafferentation mapping was discontinued in subsequent experiments. In a second rat group, designated delayed group (dAMP), rats underwent forelimb amputation and the FBS was mapped 7-to-27 wks later. Pre-deafferentation mapping was not carried out in delayed deafferents.

3.1.1 | Lower jaw-to forepaw rapid remapping following forelimb amputation (rAMP)—

New lower jaw responses were identified in the FBS examined approximately 30 min after forelimb amputation and these results are shown in Figure 2. The new lower jaw input is localized in the anterior FBS adjacent to the neighboring LJBSF, and this is illustrated in 4 rats in Figure 2(a1–a4). In one additional rat, lower jaw responsive sites were recovered in a cytochrome oxidase (CO) stained section shown in Figure 2(b) and reconstructed in Figure 2(b1). A summary of penetration sites from 7 rats, where lower jaw responses were recorded within the FBS is plotted on a template of the FBS and these results are shown in Figure 2(c). Note that the sites responsive to input from the lower jaw are localized in the anterior FBS corresponding to the locations of D1, D2, and TH barrels. However, most sites in the FBS were unresponsive to lower jaw input particularly in the posterior FBS.

3.1.2 | Lower jaw-to forepaw rapid remapping following brachial plexus nerve cut (rBPnc)—

New lower jaw responses were also observed immediately after brachial plexus nerve cut (rBPnc) and these results are illustrated in Figure 3. The responses are

again localized in the anterior FBS and shown in 4 rats (Figure 3(a1–a4)). In another rat, one lower jaw responsive site in the FBS was recovered in this FBS shown in Figure 3(b) and reconstructed in the line drawing in Figure 3(b1). The data from all rBPnc rats (n=6) are plotted on the FBS template in Figure 3(c) and illustrate the concentration of lower jaw responsive sites in the anterior FBS.

3.1.3 | Lower jaw-to forepaw rapid remapping following brachial plexus anesthesia (rBPA)—

New lower jaw responses appeared in the FBS within 30 min of delivery of an injection of lidocaine (2%) in the brachial plexus and these results are shown in Figure 4. Examples from 4 rats are shown in the left panel, Figure 4(a1–a4), where sites responsive to input from the lower jaw were again localized anteriorly in the FBS but this time displaced toward the D2 barrels. Figure 4(b1) illustrates the results from another experiment where two penetrations were recovered in the FBS that were responsive to input from the lower jaw; these results are plotted on a CO-stained section where the FBS is outlined (white dashes) and the locations of electrode penetrations within the FBS and surrounding SI are also shown. Two lower jaw responsive sites (red circles) and non-responsive sites (black circles) in the FBS are shown along with lower jaw responsive sites outside the FBS (blue circles); these results are plotted in the line drawing reconstruction in Figure 4(b1). All data collected within the FBS, from a total of 7 rats, are plotted on the template in Figure 4(c); lower jaw responsive sites (red circles) and non-responsive sites (black circles) are shown. Note again that the lower jaw responsive sites are localized anteriorly in the FBS, but fewer lower jaw responsive sites encroached on the anterior border of the FBS, and instead were displaced to the D2 barrels.

3.1.4 | Lower jaw-to forepaw delayed mapping following forelimb amputation (dAMP)—

In the delayed group, we examined the FBS between 7–27 weeks after forelimb amputation for responses from the lower jaw and these results are shown in Figure (5). Line drawing reconstructions from 4 rats are shown in Figure 5(a1–a4) along with the time in weeks of mapping after amputation. In these rats, lower jaw responsive sites were no longer restricted to the anterior FBS but rather distributed throughout the entire FBS. This distribution is also shown for the rat illustrated in Figure 5(b) and 5(b1). In Figure 5(c), a summary of the electrode penetrations for the 6 rats is plotted on the FBS template and these results present a remarkably different profile of reorganization from the rapid deafferents. In 3 rats mapped earlier than 7-weeks after amputation, responsive sites were restricted to the anterior FBS, similar to rapid deafferents (data not shown).

3.2 | Areal measures of FBS and lower jaw representation in deafferented FBS for each deafferentation group

We measured and compared the mean area of the newly expressed lower jaw representation in the deafferented FBS in rapid and delayed groups of forelimb deafferented rats (rAMP, rBPnc, rBPA, dAMP) and these results are shown in Table 1. All areal measures of the FBS were obtained from CO-stained sections; no significant differences in sizes of the FBS were found between deafferentation groups. However, inspection of the mean area of the lower jaw in the FBS and mean percent lower jaw area within the FBS was noticeably different between rapid and delayed groups, and a significantly larger area of the FBS could

be activated by stimulation of the lower jaw in the group studied after a time delay as shown in Figure 6. In addition, there were significant differences in percent area representation in the rapid deafferentation groups and these are shown in Figure 6. Inspection of Figure 6 shows that the mean percentage of the rAMP group was significantly greater than the other rapid deafferented groups while no significant differences were observed between rBPnc and rBPA groups.

3.3 | Lower jaw responsive sites within individual FBS barrels in deafferented rat groups

For each deafferentation group we counted the total number of recording sites where receptive fields of neurons were recovered within individual barrels and the percentage of those sites that were responsive to input from the lower jaw and these results are shown in Fig. 7. Inspection of the results from the three rapid deafferentation groups shows that lower jaw responses were localized in the anterior barrels. Note that the glabrous digits D2–D5 are topographically represented by 3 or 4 individual mediolaterally running barrels, while their dorsal representation lies immediately lateral in a nebulous barrel-free border. D1 dorsal and ventral are represented by single barrels as are the representation of digit and palmar pads. In contrast, a greater percentage of lower jaw responsive sites in dAMP rats are distributed throughout the entire FBS.

3.4 | Evoked response latencies in intact and deafferented FBS

Measurement of evoked response latencies can provide useful temporal information on the time it takes for a signal from the periphery to reach a target, for example SI. We examined evoked response latencies as an initial step in ascertaining possible source(s) of the newly expressed lower jaw input in the deafferented FBS. Firstly, we measured the time required for an electrical stimulus delivered to the forepaw skin surface to reach its respective forepaw site in the FBS and the time required for an electrical stimulus delivered to the lower jaw to reach its respective site in the LJBSF. We then compared these evoked response latencies with the latency for the newly expressed lower jaw input to reach the deafferented FBS and these results are shown in the bar graph in Figure 8. The mean evoked response latencies for input from the lower jaw to reach the LJBSF (6.94 ms) and for input from the forepaw to reach the FBS (7.26 ms) were not significantly different. Nonetheless, these evoked response latencies were significantly shorter than the evoked response latencies for lower jaw input to reach the FBS in all deafferentation groups. Unexpectantly, the evoked response latency of the rBPA group was significantly longer compared to all other deafferented groups.

A representative example of evoked response latencies obtained in each deafferented group is shown in Figure 9. In rapidly mapped groups (a1–a3), evoked responses recorded in the intact FBS prior to deafferentation are shown (upper row) following 25 consecutive electrical stimulations of the forepaw (Pre_{FP}); raster plot and post-stimulus time histogram (PSTH) are also shown for all stimulations. In the middle row, with the electrode remaining at the same location in the FBS as in the upper trace, 25 consecutive electrical stimulations delivered to the lower jaw and evoked responses recorded in the FBS prior to forelimb deafferentation (Pre_{LJ}) are shown along with accompanying raster plot and PSTH. In the bottom row, obtained after deafferentation, evoked responses recorded in the deafferented

FBS ($Post_{LJ}$) following 25 consecutive stimulations delivered to the lower jaw are shown along with an accompanying raster plot and PSTH. In the dAMP group (a4), evoked responses following stimulation of the lower jaw were only recorded after forelimb amputation ($Post_{LJ}$).

Inspection of the traces in rapidly deafferented groups show a robust evoked response in the intact FBS following stimulation of the forepaw, no evidence of an evoked response in the intact FBS following stimulation of the lower jaw, and a longer latency evoked response ($Post_{LJ} > Pre_{FP}$) following stimulation of the lower jaw in the deafferented FBS. In the dAMP rat, examined 10 wks after amputation, a robust evoked response is recorded in the deafferented FBS following stimulation of the lower jaw; note that no pre-amputation recording was performed in this group.

4. | DISCUSSION

Major findings

We used the FBS in adult rats as our model system to study rapid and delayed lower jaw-to-forepaw cortical reorganization. The present study extends our previous findings of delayed large-scale cortical reorganization following forelimb amputation whereby new input from the neighboring shoulder-skin surface appears in the deafferented FBS one or more months after forelimb amputation (Pearson, Li et al. 1999). Here, we report both delayed and rapid cortical reorganization following forelimb deafferentation whereby new input from the non-adjacent lower jaw skin surface appears in the deafferented FBS. The major findings of this study are: (1) immediately following forelimb deafferentations, that include forelimb amputation, brachial plexus nerve cut or brachial plexus anesthesia, new input from the lower jaw is immediately expressed in the deafferented FBS and is localized to sites in the anterior FBS; (2) in forelimb amputees mapped between 7–27 weeks after amputation, the newly expressed lower jaw input is distributed throughout both anterior and posterior parts of the FBS, and occupies a significantly larger percentage of total FBS area compared to rapidly mapped deafferents; (3) evoked response latencies recorded in the deafferented FBS following electrical stimulation of the lower jaw skin surface were significantly longer in both rapid and delayed deafferents compared to latencies for input from the forepaw to reach the FBS or for input from lower jaw to reach the LJBSF; (4) the longer latencies measured for forelimb deafferents are consistent with the notion that an additional relay is imposed along the somatosensory pathway prior to the lower jaw input expression in the deafferented FBS. In view of recent findings (de Jongh Curry, Wang et al. 2022, Wang, Pellicer-Morata et al. 2022), it is likely that different sources and mechanisms underlie rapid and delayed FBS cortical reorganization.

Technical comments –

The LJBSF consists of a somatotopic arrangement of approximately 24 barrels that are associated with the representation of chin vibrissae and microvibrissae (Pellicer-Morata, Wang et al. 2021). Deflection of individual chin vibrissae or microvibrissae was sufficient to activate cells within individual barrels. Chin vibrissae and microvibrissae are embedded in common fur that could be stimulated by brushing or lightly tapping the hairy skin surface;

the common fur on the lower jaw was also somatotopically organized as was the common fur in other barrel subfields (Rice and Munger 1986). In the present study, lower jaw responsive neurons in the deafferented FBS were driven by stimulating the common fur, but not by deflecting individual chin vibrissae or microvibrissae and likely reflects activation of both hairy skin receptors and deep receptors coded by intensity. Our stimulation technique is consistent with the descriptions of previous mapping studies of the LJBSF (Welker 1971, Welker 1976) and reorganization studies of lower jaw-to-forepaw remapping in the FBS (Hickmott and Merzenich 2002, Pluto, Lane et al. 2003, Oliveira, Bittencourt-Navarrete et al. 2014). We also stimulated the lower jaw skin surface with a bipolar stimulating electrode to examine evoked response latencies in forelimb intact and deafferented FBS, as previously described (Pearson, Li et al. 1999).

Lower jaw reorganization in rat FBS following forelimb deafferentation –

In the present study, we provided evidence for rapid (immediate) and delayed (chronic, long-term) reorganization in FBS following forelimb deafferentation. In rapid reorganization, new lower jaw input is immediately expressed in the anterior FBS while in delayed reorganization examined 7-weeks or more after forelimb amputation, lower jaw responsive sites occupy both anterior and posterior FBS. These findings for rapid and delayed groups are plotted together in Figure 10. Possible source(s) for this differential representation are discussed in a later section.

Lower jaw reorganization in rat FBS –

Loss of peripheral sensory forelimb input to rat FBS, independent of whether the loss derives from forelimb amputation, brachial plexus nerve cut, or injection of a nerve blocker in the brachial plexus, leads to immediate expression of new lower jaw input in the anterior FBS. The anterior FBS, in intact rats, as defined here, receives input from the glabrous ventral and dorsal hairy skin surfaces of D1, D2, D3, and thenar (TH) pad, digit pad one (P1) and P2 of the forepaw, while the posterior FBS receives input from glabrous and hairy skin surfaces of D4, D5, hypothenar (HT) and pad, P3, as shown in Figure 1.

We measured the area of the new lower jaw representation in the FBS for rapid and delayed deafferentation groups. The total averaged FBS area occupied by the new lower jaw input in delayed amputees (dAMP) was significantly larger compared to all rapid deafferentation groups. Significant differences in the total averaged area of the new lower jaw representation were also observed among the rapid deafferentation groups; total averaged area of new lower jaw representation in rAMP rats was significantly larger compared to rBPnc and rBPA groups. While each deafferentation type was designed to remove sensory input from the entire forelimb at the level of the brachial plexus, it is likely that the larger area of reorganization observed within the FBS in rAMP rats was related to the extent of the deafferentation where the entire forelimb was removed. In some rBPnc rats, small nerve branches may have been inadvertently spared during transection, and in rBPA rats, infiltration of the nerve block may have been incomplete although the location of the injection site(s) on the skin surface, injection depth, and the volume of blocker were identical to a previous report (Zhang, Cui et al. 2019). Thus, a relationship likely exists

between the extent of the deafferentation and the resulting areal size of the lower jaw reorganization in the FBS.

Lower jaw-to-forepaw reorganization has received scant attention in rat, and in those studies where lower jaw responses were reported in forepaw SI following peripheral deafferentation (Hickmott and Merzenich 2002, Pluto, Lane et al. 2003, Oliveira, Bittencourt-Navarrete et al. 2014), none related the locations of the new lower jaw responsive sites to the underlying barrels in the FBS, measured the area of the new representation or measured evoked responses latency of the new input.

– Rapid lower jaw reorganization – Oliveira and colleagues examined reorganization of the FBS, as part of a nerve regeneration study, and reported in control rats that new input from the lower lip (lower jaw) invaded the FBS immediately after brachial plexus nerve cut that included radial, ulnar, and median nerves (Oliveira, Bittencourt-Navarrete et al. 2014). The new lower lip input occupied a narrow shell at the anterior border of the FBS adjacent to the posterior LJBSF; from their Figure 7, the new input appeared to occupy sites in the former D1 and TH representation. Their findings are similar to our rBPnc rats that underwent brachial plexus nerve cut and immediately expressed new lower jaw responses in the deafferented FBS. However, in our study, new lower jaw input was also found in D1–D3 and TH barrels.

Rapid expansion of new lower jaw input in the deafferented FBS was also demonstrated by examining changes in the location of FBS/LJBSF border following peripheral nerve cut (Hickmott and Merzenich 2002). These investigators identified a physiological border between the LJBSF and FBS in forelimb intact rats where neurons were responsive to input from both the forepaw and lower jaw; next, they transected the radial and medial peripheral nerves and reported that the physiological border acutely expanded into the anterior FBS where it was confined to a shell-like region adjacent to the LJBSF. Examination at days 7 thorough 28 showed the border occupied a larger area of the FBS that appeared confined to the anterior FBS (Hickmott and Merzenich 2002). Our results for rBPnc rats, where radial, ulnar, and median nerves were cut, show a similar rapid pattern of lower jaw input in the anterior FBS.

Rapid reorganization was reported in the rat hindpaw barrel subfield (HBS) following hindlimb nerve transection (Wall and Cusick 1984), hindlimb digit denervation (Byrne and Calford 1991) and in the FBS following thoracic transection of the spinal cord (Aguilar, Humanes-Valera et al. 2010). In both hindlimb peripheral deafferentation studies (Wall and Cusick 1984, Byrne and Calford 1991) the resulting reorganization was restricted to the HBS and did not result in reorganization in the neighboring FBS. Rapid reorganization in SI was also reported in flying fox following digit denervation, but whether the reorganization also included new input from the face in the deafferented digit cortex was not indicated (Calford and Tweedale 1988, Calford and Tweedale 1991). Similarly, single digit amputation in raccoon, results in immediate input from surrounding digits in the deafferented digit cortex but not from lower jaw or hindlimb (Rasmusson and Turnbull 1983, Kelahan and Doetsch 1984).

– Delayed lower jaw reorganization – Lower jaw responsive sites were reported in the FBS in adult rats mapped 2 or more months after a mid-shaft section of the humerus (Pluto, Lane et al. 2003). These investigators reported that the majority of sites in the deafferented FBS were responsive to input from the forelimb-stump, while a smaller percentage of recording sites (10%) received input from the face and lower jaw (Pluto, Lane et al. 2003). Our results from forelimb amputees (dAMP), mapped 7 or more weeks after forelimb amputation, are similar in that lower jaw responsive sites were identified in the FBS, but differed in respect to the extensive distribution of lower jaw input throughout the entire deafferented FBS observed in the present study (see Figs. 5 and 10). Several possible explanations for this discrepancy exist. Firstly, the nature and extent of the amputation differs between studies; we removed the forelimb at the glenno-humeral joint, while they amputated the forelimb at the mid-humerus leaving a residual upper limb and stump. Secondly, they reported that the predominate input in the deafferented FBS derived from stump and remaining residual limb, which may serve to mask input from face and lower lip while we identified approximately 60% of the total FBS responded to new input from the lower jaw. Still other investigators reported a largely silent FBS in rats mapped 13 or more weeks after an elbow-level amputation (Marasco and Kuiken 2010); however, this finding is difficult to reconcile with the Pluto study and present results.

Reorganization in the FBS –

In the rodent barrel field, the FBS is bordered in serial order by the representations of the forearm, upper arm, and shoulder (Welker 1976, Pearson, Li et al. 1999), and anterolaterally by the representation of the lower jaw and chin in the LJBSF (Pellicer-Morata, Wang et al. 2021). Within the somatotopically organized FBS, digits 2–5 are represented by columns of 3-to-4 mediolateral-running barrels (see Fig. 1). One month after amputating D3, neurons formerly associated with the representation of D3 become responsive to input from neighboring digits D2 and D4 and the remaining stump (McCandlish et al 1996). In a later study, we reported that 6–16 weeks after forelimb amputation, two or more islets of new shoulder representation appeared in the deafferented FBS, and evoked response latencies recorded from the islets were significantly longer compared to evoked response latencies for input from the shoulder to reach its “original” shoulder representation in the posterior barrel field (Pearson, Li et al. 1999). The “original” shoulder representation is located approximately 3 mm posterior to the FBS (Pearson, Li et al. 1999) compared to the approximately 200-300 μm distance of the LJBSF (Hickmott and Merzenich 2002). In the present study, new lower jaw responses were recorded in the anterior FBS immediately following forelimb amputation but required 7 or more post-amputation weeks to populate the entire FBS. The longer time-period for new shoulder input to reach the deafferented FBS is similar to the time period for new lower jaw input to reach the posterior FBS and may involve similar mechanisms discussed later.

Lower jaw reorganization in forelimb SI in other species

Cortical reorganization was first reported in cat SI when forelimb nerves that innervated the paw cortex were transected and 8–10 weeks later the deafferented paw cortex became responsive to new input from the forearm (Kalaska and Pomeranz 1979). Subsequent reorganization studies carried out in adult monkeys depriving SI of their normal forelimb

inputs following transection of peripheral nerve(s) (Kaas, Merzenich et al. 1983, Merzenich, Kaas et al. 1983a, Merzenich, Kaas et al. 1983b) or digit amputation (Merzenich, Nelson et al. 1984) and SI examined weeks or months later resulted in neighboring skin regions gaining access to the deafferented SI. In these studies, the limited reorganization observed from neighboring skin regions was hypothesized to result from overlapping thalamocortical axon terminals, such as when the principal input was removed by peripheral deafferentation, the remaining overlapping thalamocortical input(s) became expressed in the deactivated SI. The limitation hypothesis worked-well for single peripheral nerve transection and/or single digit amputation, but was challenged by later deafferentation studies that deprived larger regions of forelimb SI by extensive peripheral nerve transection (Garraghty and Kaas 1991) or dorsal root spinal transection (Pons, Garraghty et al. 1991). Following transection of median and ulnar nerves in adult squirrel monkeys, a large area of hand SI was deprived of input which completely regained cutaneous responsiveness 2–5 months after transection (Garraghty and Kaas 1991). In their seminal study, Pons and colleagues (Pons, Garraghty et al. 1991) physiologically mapped the former upper limb representation in SI in macaque monkeys that underwent a dorsal rhizotomy severing dorsal root spinal segments (C2–C4) twelve years earlier and reported massive new input from the chin and lower jaw had completely occupied the deafferented SI. Face/lower jaw-to-hand remapping in SI of monkey was subsequently reported following deafferentations that included dorsal column lesion (Jain, Catania et al. 1997, Jain, Florence et al. 2000, Jain, Qi et al. 2008, Tandon, Kambi et al. 2009), hand forelimb amputation (Florence, Hackett et al. 2000), but in each of these studies, new lower jaw input in the forelimb deafferented SI was reported months to years following deafferentation. In a more recent report, there was no immediate reorganization in the ventral posterior nucleus or area 3b following a lesion in the dorsal column, although after 6 months, new face responsive sites were reported in both locations (Jain, Qi et al. 2008).

Source(s) and mechanism(s) of lower jaw to forepaw reorganization

In this study, we present our findings that stimulation of the lower jaw, in forelimb deafferented rats, immediately induces new lower jaw responses in the FBS that are not observed in rats with intact forelimbs. This suggests that there is pre-existing lower jaw input before deafferentation but is inhibited from being expressed (Rasmusson and Turnbull 1983, Dykes and Lamour 1988, Calford and Tweedale 1991, Calford and Tweedale 1991, Dykes 1997). By using anterograde and retrograde tracers, we identified a fiber pathway between the lower jaw barrel subfield (LJBSF) and the anterior FBS in both intact and deafferented rats (Wang, Pellicer-Morata et al. 2022). This pathway may serve as a substrate for the suppressed lower jaw input. Previously, researchers reported a similar cortical connection between the LJBSF and anterior FBS in rats (Fabri and Burton 1991). Furthermore, we found that injecting bicuculline methiodide (BMI), a $GABA_A$ blocker, into the FBS of intact rats quickly revealed lower jaw responses in the anterior FBS (de Jongh Curry, Wang et al. 2022). This suggests that the LJBSF may be a potential source of lower jaw input that is normally inhibited by GABAergic inhibition. In intact monkeys, corticocortical connections between the face representation in SI and the neighboring hand representation have been reported (Manger, Woods et al. 1997, Chand and Jain 2015). However, it is unknown whether this projection pathway leads to immediate reorganization

of the lower jaw. Alternatively, it is possible that thalamocortical afferents from the lower jaw representation in the ventral posterior medial nucleus (VPM) could send branches to the forelimb SI, providing an additional source of lower jaw reorganization. However, there is currently no anatomical evidence supporting this possibility in both intact and forelimb deafferented animals (Chand and Jain 2015, Wang, Pellicer-Morata et al. 2022).

The origin of the observed lower jaw input in the posterior FBS of dAMP rats remains unknown, and there is currently no evidence supporting an origin in LJBSF (Wang, Pellicer-Morata et al. 2022). In a related study, we found that new shoulder responses emerged in the FBS after a period of six weeks or more following forelimb amputation (Pearson, Li et al. 1999). Interestingly, these new shoulder responses did not stem from the “original” shoulder representation in the posterior barrel field (Pearson, Arnold et al. 2001). Instead, it is likely that they originated from a functionally reorganized ventral posterior lateral nucleus (VPL), where neurons in the former digit representation acquired responsiveness to input from the shoulder; this shoulder-related information is then relayed to the deafferented FBS (Li, Chappell et al. 2014). Building upon this finding, we propose that the lower jaw input observed in the posterior FBS of dAMP rats might also stem from a reorganized VPL. In this scenario, cells in the previous digit representation within the VPL would acquire responsiveness to new lower jaw input, which would subsequently be transmitted to the deafferented FBS.

Reorganization in VPL occurs over an extended period, ranging from months to years, following central or peripheral damage to the forelimb and/or forelimb pathway (Jones and Pons 1998, Kaas, Florence et al. 1999, Florence, Hackett et al. 2000, Jain, Qi et al. 2008). In these instances, the VPL undergoes changes that make it responsive to new input from the lower jaw. An early study conducted on monkeys that had undergone dorsal rhizotomy two decades earlier revealed several noteworthy observations (Jones and Pons 1998). The investigators noted a reduction in the size of VPL, degeneration of thalamocortical cell bodies and axons, migration of neighboring VPM into the shrunken VPL, and a predominant responsiveness of the remaining VPL neurons to input from the lower jaw. Based on the extensive cortical reorganization observed in SI of these monkeys (Pons, Garraghty et al. 1991), Jones and Pons proposed a hypothesis that thalamocortical axons originating from VPM might already occupy some sites within the former SI hand representation. These sites subsequently become more active in the absence or diminished presence of forelimb input from the degenerating VPL thalamocortical axons. Another possibility is that thalamocortical cells in VPM could emit side branches, carrying input from the lower jaw to the hand/forelimb representation in SI. Additionally, it is plausible that VPM and VPL share an intra-thalamic pathway consisting of silent synapses. These synapses remain inactive until deafferentation occurs, at which point they become activated and contribute to the transmission of sensory information between nuclei. Silent synapses may indicate the presence of subthreshold input that reaches the firing threshold following a decrease in GABAergic inhibition (Li, Callaway et al. 2002).

Sprouting of corticocortical and/or brainstem connections provide other possible sources for face-to-hand reorganization. The sprouting of corticocortical and/or brainstem connections presents alternative potential sources for the reorganization of face-to-hand representations.

A study documented the sprouting of afferents between the face and hand representations in the primary somatosensory cortex (SI) of monkeys that had experienced forelimb amputation a decade earlier (Florence, Taub et al. 1998). However, other researchers have highlighted the limitations of sprouting afferents in crossing the boundary between the normal and deafferented cortex (Dykes, Avendano et al. 1995). On the contrary, some studies have shown the existence of a connection between the face and hand representations in SI of intact monkeys (Manger, Woods et al. 1997, Chand and Jain 2015) that bears similarity to the connections observed in the deafferented state (Chand and Jain 2015).

In non-human primates, researchers have observed the sprouting of face afferents from the trigeminal nucleus into the cuneate nucleus (Jain, Florence et al. 2000). This phenomenon occurs six or more years after the sectioning of dorsal columns. Moreover, cuneate neurons have been found to respond to input from the lower jaw following dorsal column section (Kambi, Halder et al. 2014, Halder, Kambi et al. 2018). Additional evidence suggests that brainstem sprouting may play a more significant role in the reorganization of SI (Kambi, Halder et al. 2014). When the lower jaw representation in monkey SI is deactivated, it fails to eliminate lower jaw input in the adjacent deafferented hand representation. However, when the cuneate nucleus is inactivated, the lower jaw input is abolished. Overall, these findings indicate that while sprouting of face afferents from the trigeminal nucleus into the cuneate nucleus and the reorganization of SI contribute to the processing of lower jaw input, the brainstem's involvement appears to be particularly crucial in mediating this phenomenon.

Rapid reorganization of the cuneate nucleus has also been reported following transection of ulnar and median nerves (Xu and Wall 1997). In these instances, cuneate neurons immediately exhibit responsiveness to input from the adjacent dorsal digits and, to a lesser extent, from skin surfaces on the forelimb, shoulder, neck, and face. However, it is currently unknown whether input from these skin surfaces is also immediately expressed in the VPL or the anterior FBS.

The source of lower jaw input in the posterior FBS has yet to be determined. Its delayed appearance, absence of a known projection from the lower jaw barrel subfield (LJBSF), and uncertainty regarding the role played by VPL suggest further investigation is required. Nonetheless, it is possible that downstream changes in the brainstem will be found to play a key role in this reorganization process.

Acknowledgments

This work is dedicated to the memory of Drs. Hiroshi Asanuma and William A. Wilson, Jr – (RSW). This work is supported by NIH grant HD 094588 (J.W.T and R.S.W.).

Funding information:

Research supported by the Eunice Kennedy Shriver National Institute of Child Health & Human Development of the National Institutes of Health under Award Number R01HD094588.

Data Availability Statement:

The data that support the findings of this study are available on request from the corresponding author.

REFERENCES

Aguilar J, Humanes-Valera D, Alonso-Calvino E, Yague JG, Moxon KA, Oliviero A and Foffani G (2010). “Spinal cord injury immediately changes the state of the brain.” J Neurosci 30(22): 7528–7537. [PubMed: 20519527]

Byrne JA and Calford MB (1991). “Short-term expansion of receptive fields in rat primary somatosensory cortex after hindpaw digit denervation.” Brain Res 565(2): 218–224. [PubMed: 1842695]

Calford MB (2002). “Dynamic representational plasticity in sensory cortex.” Neuroscience 111(4): 709–738. [PubMed: 12031401]

Calford MB and Tweedale R (1988). “Immediate and chronic changes in responses of somatosensory cortex in adult flying-fox after digit amputation.” Nature 332(6163): 446–448. [PubMed: 3352742]

Calford MB and Tweedale R (1991). “Acute changes in cutaneous receptive fields in primary somatosensory cortex after digit denervation in adult flying fox.” J Neurophysiol 65(2): 178–187. [PubMed: 2016636]

Calford MB and Tweedale R (1991). “Immediate expansion of receptive fields of neurons in area 3b of macaque monkeys after digit denervation.” Somatosens Mot Res 8(3): 249–260. [PubMed: 1767621]

Chand P and Jain N (2015). “Intracortical and Thalamocortical Connections of the Hand and Face Representations in Somatosensory Area 3b of Macaque Monkeys and Effects of Chronic Spinal Cord Injuries.” J Neurosci 35(39): 13475–13486. [PubMed: 26424892]

Collins KL, Russell HG, Schumacher PJ, Robinson-Freeman KE, O’Conor EC, Gibney KD, Yambem O, Dykes RW, Waters RS and Tsao JW (2018). “A review of current theories and treatments for phantom limb pain.” J Clin Invest 128(6): 2168–2176. [PubMed: 29856366]

de Jongh Curry A, Wang L, Tsao JW and Waters RS (2022). “Removal of GABAergic inhibition unmasks input from lower jaw barrel subfield (LJBSF) to forepaw barrel subfield (FBS) in rat primary somatosensory cortex (SI)“ Program No. 466.18. 2022 Neuroscience Meeting Planner. San Diego, CA: Society for Neuroscience, 2022. Online.

Dykes RW (1997). “Mechanisms controlling neuronal plasticity in somatosensory cortex.” Can J Physiol Pharmacol 75(5): 535–545. [PubMed: 9250389]

Dykes RW, Avendano C and Leclerc SS (1995). “Evolution of cortical responsiveness subsequent to multiple forelimb nerve transections: an electrophysiological study in adult cat somatosensory cortex.” J Comp Neurol 354(3): 333–344. [PubMed: 7608325]

Dykes RW and Lamour Y (1988). “An electrophysiological laminar analysis of single somatosensory neurons in partially deafferented rat hindlimb granular cortex subsequent to transection of the sciatic nerve.” Brain Res 449(1–2): 1–17. [PubMed: 3293700]

Elbert T, Flor H, Birbaumer N, Knecht S, Hampson S, Larbig W and Taub E (1994). “Extensive reorganization of the somatosensory cortex in adult humans after nervous system injury.” Neuroreport 5(18): 2593–2597. [PubMed: 7696611]

Fabri M and Burton H (1991). “Ipsilateral cortical connections of primary somatic sensory cortex in rats.” J Comp Neurol 311(3): 405–424. [PubMed: 1720147]

Faggin BM, Nguyen KT and Nicolelis MA (1997). “Immediate and simultaneous sensory reorganization at cortical and subcortical levels of the somatosensory system.” Proc Natl Acad Sci U S A 94(17): 9428–9433. [PubMed: 9256499]

Flor H, Elbert T, Knecht S, Wienbruch C, Pantev C, Birbaumer N, Larbig W and Taub E (1995). “Phantom-limb pain as a perceptual correlate of cortical reorganization following arm amputation.” Nature 375(6531): 482–484. [PubMed: 7777055]

Florence SL, Hackett TA and Strata F (2000). “Thalamic and cortical contributions to neural plasticity after limb amputation.” J Neurophysiol 83(5): 3154–3159. [PubMed: 10805710]

Florence SL, Taub HB and Kaas JH (1998). “Large-scale sprouting of cortical connections after peripheral injury in adult macaque monkeys.” Science 282(5391): 1117–1121. [PubMed: 9804549]

Garraghty PE and Kaas JH (1991). “Large-scale functional reorganization in adult monkey cortex after peripheral nerve injury.” Proc Natl Acad Sci U S A 88(16): 6976–6980. [PubMed: 1871112]

Haider P, Kambi N, Chand P and Jain N (2018). “Altered Expression of Reorganized Inputs as They Ascend From the Cuneate Nucleus to Cortical Area 3b in Monkeys With Long-Term Spinal Cord Injuries.” Cereb Cortex 28(11): 3922–3938. [PubMed: 29045569]

Hickmott PW and Merzenich MM (2002). “Local circuit properties underlying cortical reorganization.” J Neurophysiol 88(3): 1288–1301. [PubMed: 12205150]

Jain N, Catania KC and Kaas JH (1997). “Deactivation and reactivation of somatosensory cortex after dorsal spinal cord injury.” Nature 386(6624): 495–498. [PubMed: 9087408]

Jain N, Florence SL, Qi HX and Kaas JH (2000). “Growth of new brainstem connections in adult monkeys with massive sensory loss.” Proc Natl Acad Sci U S A 97(10): 5546–5550. [PubMed: 10779564]

Jain N, Qi HX, Collins CE and Kaas JH (2008). “Large-scale reorganization in the somatosensory cortex and thalamus after sensory loss in macaque monkeys.” J Neurosci 28(43): 11042–11060. [PubMed: 18945912]

Jones EG and Pons TP (1998). “Thalamic and brainstem contributions to large-scale plasticity of primate somatosensory cortex.” Science 282(5391): 1121–1125. [PubMed: 9804550]

Kaas JH, Florence SL and Jain N (1999). “Subcortical contributions to massive cortical reorganizations.” Neuron 22(4): 657–660. [PubMed: 10230786]

Kaas JH, Merzenich MM and Killackey HP (1983). “The reorganization of somatosensory cortex following peripheral nerve damage in adult and developing mammals.” Annu Rev Neurosci 6: 325–356. [PubMed: 6340591]

Kaas JH, Nelson RJ, Sur M, Lin CS and Merzenich MM (1979). “Multiple representations of the body within the primary somatosensory cortex of primates.” Science 204(4392): 521–523. [PubMed: 107591]

Kalaska J and Pomeranz B (1979). “Chronic paw denervation causes an age-dependent appearance of novel responses from forearm in “paw cortex” of kittens and adult cats.” J Neurophysiol 42(2): 618–633. [PubMed: 422979]

Kambi N, Halder P, Rajan R, Arora V, Chand P, Arora M and Jain N (2014). “Large-scale reorganization of the somatosensory cortex following spinal cord injuries is due to brainstem plasticity.” Nat Commun 5: 3602. [PubMed: 24710038]

Kelahan AM and Doetsch GS (1984). “Time-dependent changes in the functional organization of somatosensory cerebral cortex following digit amputation in adult raccoons.” Somatosens Res 2(1): 49–81. [PubMed: 6505463]

Li CX, Callaway JC and Waters RS (2002). “Removal of GABAergic inhibition alters subthreshold input in neurons in forepaw barrel subfield (FBS) in rat first somatosensory cortex (SI) after digit stimulation.” Exp Brain Res 145(4): 411–428. [PubMed: 12172653]

Li CX, Chappell TD, Ramshur JT and Waters RS (2014). “Forelimb amputation-induced reorganization in the ventral posterior lateral nucleus (VPL) provides a substrate for large-scale cortical reorganization in rat forepaw barrel subfield (FBS).” Brain Res 1583: 89–108. [PubMed: 25058605]

Manger PR, Woods TM, Munoz A and Jones EG (1997). “Hand/face border as a limiting boundary in the body representation in monkey somatosensory cortex.” J Neurosci 17(16): 6338–6351. [PubMed: 9236243]

Marasco PD and Kuiken TA (2010). “Amputation with median nerve redirection (targeted reinnervation) reactivates forepaw barrel subfield in rats.” J Neurosci 30(47): 16008–16014. [PubMed: 21106839]

McCandlish C, Waters RS and Cooper NG (1989). “Early development of the representation of the body surface in SI cortex barrel field in neonatal rats as demonstrated with peanut agglutinin

binding: evidence for differential development within the rattunculus." Exp Brain Res 77(2): 425–431. [PubMed: 2792289]

McCandlish CA, Li CX and Waters RS (1993). "Early development of the SI cortical barrel field representation in neonatal rats follows a lateral-to-medial gradient: an electrophysiological study." Exp Brain Res 92(3): 369–374. [PubMed: 8454002]

McCandlish CA, Li CX, Waters RS and Howard EM (1996). "Digit removal leads to discrepancies between the structural and functional organization of the forepaw barrel subfield in layer IV of rat primary somatosensory cortex." Exp Brain Res 108(3): 417–426. [PubMed: 8801121]

McKinley PA, Jenkins WM, Smith JL and Merzenich MM (1987). "Age-dependent capacity for somatosensory cortex reorganization in chronic spinal cats." Brain Res 428(1): 136–139. [PubMed: 3815108]

Merzenich MM, Kaas JH, Wall J, Nelson RJ, Sur M and Felleman D (1983a). "Topographic reorganization of somatosensory cortical areas 3b and 1 in adult monkeys following restricted deafferentation." Neuroscience 8(1): 33–55. [PubMed: 6835522]

Merzenich MM, Kaas JH, Wall JT, Sur M, Nelson RJ and Felleman DJ (1983b). "Progression of change following median nerve section in the cortical representation of the hand in areas 3b and 1 in adult owl and squirrel monkeys." Neuroscience 10(3): 639–665. [PubMed: 6646426]

Merzenich MM, Nelson RJ, Stryker MP, Cynader MS, Schoppmann A and Zook JM (1984). "Somatosensory cortical map changes following digit amputation in adult monkeys." J Comp Neurol 224(4): 591–605. [PubMed: 6725633]

Oliveira JT, Bittencourt-Navarrete RE, de Almeida FM, Tonda-Turo C, Martinez AM and Franca JG (2014). "Enhancement of median nerve regeneration by mesenchymal stem cells engraftment in an absorbable conduit: improvement of peripheral nerve morphology with enlargement of somatosensory cortical representation." Front Neuroanat 8: 111. [PubMed: 25360086]

Pearson PP, Arnold PB, Oladehin A, Li CX and Waters RS (2001). "Large-scale cortical reorganization following forelimb deafferentation in rat does not involve plasticity of intracortical connections." Exp Brain Res 138(1): 8–25. [PubMed: 11374086]

Pearson PP, Li CX and Waters RS (1999). "Effects of large-scale limb deafferentation on the morphological and physiological organization of the forepaw barrel subfield (FBS) in somatosensory cortex (SI) in adult and neonatal rats." Exp Brain Res 128(3): 315–331. [PubMed: 10501804]

Pearson PP, Oladehin A, Li CX, Johnson EF, Weeden AM, Daniel CH and Waters RS (1996). "Relationship between representation of hindpaw and hindpaw barrel subfield (HBS) in layer IV of rat somatosensory cortex." Neuroreport 7(14): 2317–2323. [PubMed: 8951845]

Pellicer-Morata V, Wang L, de Jongh Curry A, Tsao JW and Waters RS (2021). "Structural and functional organization of the lower jaw barrel subfield in rat primary somatosensory cortex." J Comp Neurol 529(8): 1895–1910. [PubMed: 33135168]

Pluto CP, Lane RD, Chiaia NL, Stojic AS and Rhoades RW (2003). "Role of development in reorganization of the SI forelimb-stump representation in fetally, neonatally, and adult amputated rats." J Neurophysiol 90(3): 1842–1851. [PubMed: 12773492]

Pons TP, Garraghty PE, Ommaya AK, Kaas JH, Taub E and Mishkin M (1991). "Massive cortical reorganization after sensory deafferentation in adult macaques." Science 252(5014): 1857–1860. [PubMed: 1843843]

Pons TP, Wall JT, Garraghty PE, Cusick CG and Kaas JH (1987). "Consistent features of the representation of the hand in area 3b of macaque monkeys." Somatosens Res 4(4): 309–331. [PubMed: 3589287]

Ramachandran VS, Stewart M and Rogers-Ramachandran DC (1992). "Perceptual correlates of massive cortical reorganization." Neuroreport 3(7): 583–586. [PubMed: 1421112]

Rasmusson DD (1982). "Reorganization of raccoon somatosensory cortex following removal of the fifth digit." J Comp Neurol 205(4): 313–326. [PubMed: 7096623]

Rasmusson DD and Turnbull BG (1983). "Immediate effects of digit amputation on SI cortex in the raccoon: unmasking of inhibitory fields." Brain Res 288(1–2): 368–370. [PubMed: 6661627]

Rasmusson DD, Turnbull BG and Leech CK (1985). “Unexpected reorganization of somatosensory cortex in a raccoon with extensive forelimb loss.” Neurosci Lett 55(2): 167–172. [PubMed: 4000544]

Rice FL and Munger BL (1986). “A comparative light microscopic analysis of the sensory innervation of the mystacial pad. II. The common fur between the vibrissae.” J Comp Neurol 252(2): 186–205. [PubMed: 3782507]

Rothman JS and Silver RA (2018). “NeuroMatic: An Integrated Open-Source Software Toolkit for Acquisition, Analysis and Simulation of Electrophysiological Data.” Front Neuroinform 12: 14. [PubMed: 29670519]

Tandon S, Kambi N, Lazar L, Mohammed H and Jain N (2009). “Large-scale expansion of the face representation in somatosensory areas of the lateral sulcus after spinal cord injuries in monkeys.” J Neurosci 29(38): 12009–12019. [PubMed: 19776287]

Wall JT and Cusick CG (1984). “Cutaneous responsiveness in primary somatosensory (S-I) hindpaw cortex before and after partial hindpaw deafferentation in adult rats.” J Neurosci 4(6): 1499–1515. [PubMed: 6726345]

Wang L, Pellicer-Morata V, de Jongh Curry A, Tsao JW and Waters RS (2022). “Lower jaw barrel subfield (LJBSF) in rat somatosensory cortex provides a source of lower jaw input in the anterior forepaw barrel subfield (FBS) immediately following forelimb deafferentation.” Program No. 466.17. 2022 Neuroscience Meeting Planner. San Diego, CA: Society for Neuroscience, 2022. Online.

Waters RS, Li CX and McCandlish CA (1995). “Relationship between the organization of the forepaw barrel subfield and the representation of the forepaw in layer IV of rat somatosensory cortex.” Exp Brain Res 103(2): 183–197. [PubMed: 7789426]

Waters RS, McCandlish CA and Cooper NG (1990). “Early development of SI cortical barrel subfield representation of forelimb in normal and deafferented neonatal rat as delineated by peroxidase conjugated lectin, peanut agglutinin (PNA).” Exp Brain Res 81(2): 234–240. [PubMed: 1697807]

Welker C (1971). “Microelectrode delineation of fine grain somatotopic organization of (SmI) cerebral neocortex in albino rat.” Brain Res 26(2): 259–275. [PubMed: 4100672]

Welker C (1976). “Receptive fields of barrels in the somatosensory neocortex of the rat.” J Comp Neurol 166(2): 173–189. [PubMed: 770516]

Xu J and Wall JT (1997). “Rapid changes in brainstem maps of adult primates after peripheral injury.” Brain Res 774(1–2): 211–215. [PubMed: 9452211]

Yang TT, Gallen C, Schwartz B, Bloom FE, Ramachandran VS and Cobb S (1994a). “Sensory maps in the human brain.” Nature 368(6472): 592–593. [PubMed: 8145842]

Yang TT, Gallen CC, Ramachandran VS, Cobb S, Schwartz BJ and Bloom FE (1994b). “Noninvasive detection of cerebral plasticity in adult human somatosensory cortex.” Neuroreport 5(6): 701–704. [PubMed: 8199341]

Zhang Y, Cui B, Gong C, Tang Y, Zhou J, He Y, Liu J and Yang J (2019). “A rat model of nerve stimulator-guided brachial plexus blockade.” Lab Anim 53(2): 160–168. [PubMed: 30049253]

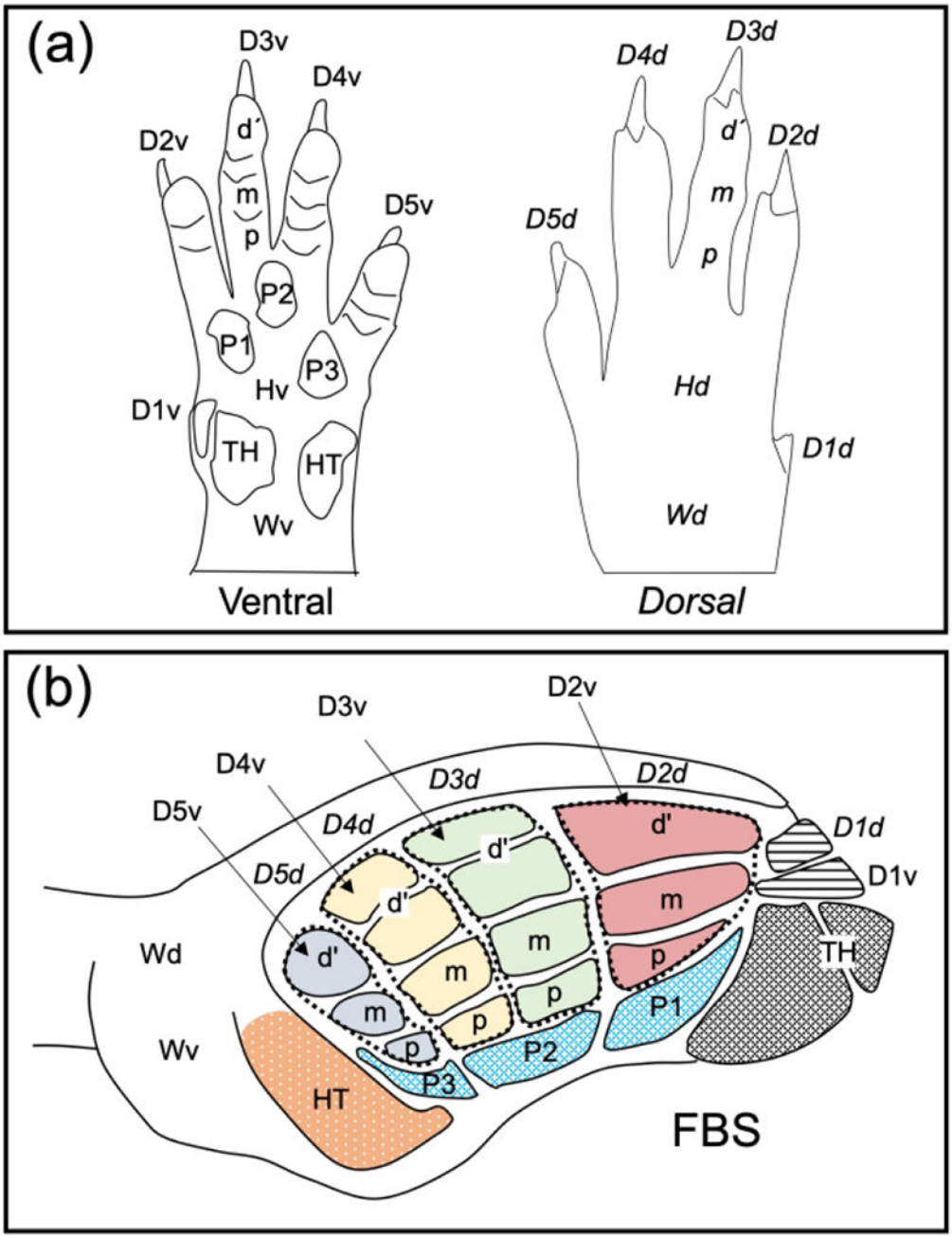

FIGURE 1.

The forepaw barrel subfield (FBS) serves as our template to summarize results of lower jaw-to-forepaw remapping following forelimb deafferentation. The rat forepaw consists of glabrous ventral and hairy dorsal skin surfaces and a line drawing illustrating these surface features, along with nomenclature designating individual digit and pad regions, is illustrated in Figure 1(a). The ventral glabrous surface contains digit two (D2v) through D5v, a small D1v, three underlying digit pads (P1–P3), and well-demarcated thenar (TH) and hypothenar (HT) pads. The dorsal surface is covered by hairy skin overlying *D1d* through *D5d*, a

dorsal hairy hand region (*Hd*), and a dorsal wrist region (*Wd*). The forepaw skin surface is represented in the FBS, and this subfield is reconstructed in the line-drawing in Figure 1(b). Four mediolaterally running rows of barrel-bands (dashed lines) can be seen that represent glabrous digits *D2d–D5d*); each barrel band is further divided into distal (d'), middle (m), and proximal regions. The representations of digit pads, pad one (P1) through P3, located beneath the four-barrel bands, and thenar (TH) and hypothenar pads are also shown. The dorsal surface of D1 (*D1d*) and the ventral surface of D1 (D1v) are represented by single barrels in the rostral-most part of the FBS. The dorsal hairy digit skin is represented by a lateral strip overlying the glabrous barrels and designated as *D2d* through *D5d*, overlying their respective barrel bands. Adapted from Waters et al. 1995.

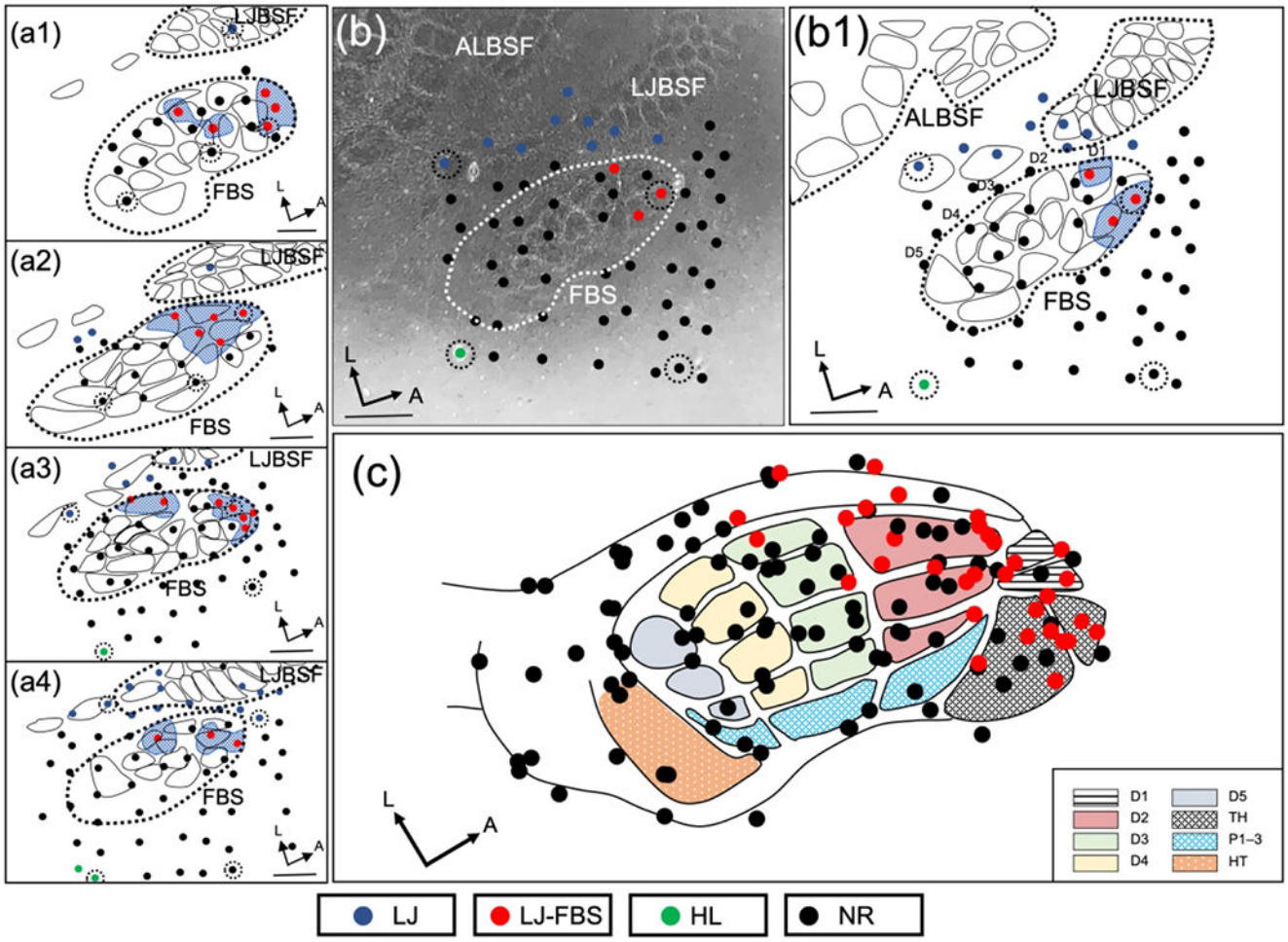

FIGURE 2.

Representation of lower jaw in deafferented FBS – rapid amputee group (rAMP). (a1–a4) Representative examples of reconstructed physiological maps of four rAMP rats, mapped immediately after forelimb amputation. Solid circles indicate electrode penetration sites where receptive fields were examined. Locations of lower jaw responsive sites in the deafferented FBS (LJ-FBS) are shown by red circles and the area encompassing these sites within the FBS is enclosed with blue stippling. Lesion sites are designated with black-dashed circular lines surrounding a recording site. Non-responsive recording sites (NR), where lower jaw responses were not found within the FBS, are designated by black circles; lower jaw responsive sites outside the FBS are designated with blue circles and hindlimb responsive sites are shown with green circles. (b) Photomicrograph of a CO-stained flattened and tangentially cut section; FBS is enclosed by a white dashed line and the lower jaw responsive sites within the FBS are shown with red circles. Non-responsive penetration sites are indicated by black circles; lower jaw responsive sites outside the FBS are designated with blue circles and the location of a hindlimb responsive site is indicated with a green circle. (b1) Line drawing reconstruction from (b) showing all recording sites in the FBS; lower jaw responsive sites are indicated with red circles, and non-responsive sites are indicated with black circles. Recording sites surrounding the FBS are also shown. (c)

Composite reconstruction of lower jaw responsive sites from seven rAMP rats are fitted on to the FBS template; red circles indicate locations of lower jaw responsive sites and black circles show non-responsive sites. FBS nomenclature shown in box at lower right. Digit one (D1) through D5, thenar pad (TH), digit pads (P1–P3), hypothenar pad (HT), lower jaw (LJ), lower jaw recording sites in FBS (LJ-FBS), hindlimb (HL), no-response (NR). Lower jaw barrel subfield: LJBSF; Anterior Lateral Barrel Subfield: ALBSF. Scale bars = 1 mm.

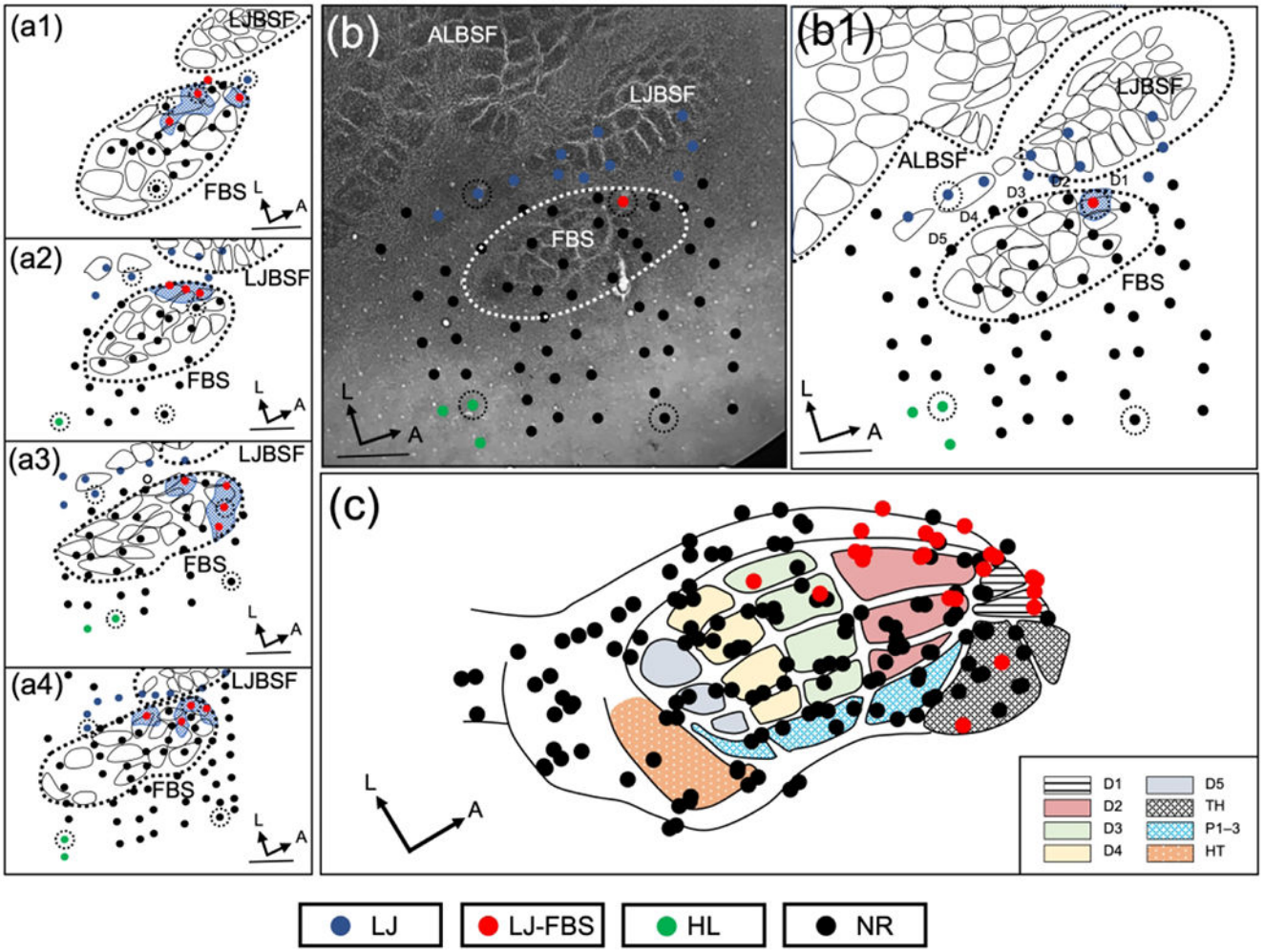

FIGURE 3.

Representation of lower jaw in the deafferented FBS – rapid brachial plexus nerve cut group (rBPnc). (a1–a4) Representative examples of reconstructed physiological maps of four rBPnc rats, mapped immediately after nerve cut. Lower jaw responsive sites in deafferented FBS (LJ-FBS) are shown by red circles and their areas within the FBS are enclosed by blue stippling. Lesion sites are designated with black-dashed circular lines around a recording site. Non-responsive sites (NR) where lower jaw responses were not found are designated by black circles; lower jaw responsive sites outside the FBS are indicated with blue circles and hindlimb (HL) responsive sites are designated with green circles. (b) Photomicrograph of a CO-stained flattened and tangentially cut section; FBS is enclosed by white dashed line and a lower jaw responsive site within the FBS is shown with a red circle. (b1) Line drawing reconstruction from (b) showing lower jaw responsive site (red circle) and non-responsive sites (black circles) in the FBS. (c) Composite reconstruction of lower jaw responsive sites from seven rBPnc rats are fitted on the FBS template; lower jaw responsive sites (red circles), non-responsive sites (black circles). FBS nomenclature shown in box at lower right. Digit one (D1) through D5, thenar pad (TH), digit pads (P1–P3), hypothenar pad (HT), lower jaw (LJ), lower jaw recording sites in FBS (LJ-FBS), hindlimb (HL), no-response

(NR). Lower jaw barrel subfield: LJBSF; Anterior Lateral Barrel Subfield: ALBSF. Scale bars = 1 mm.

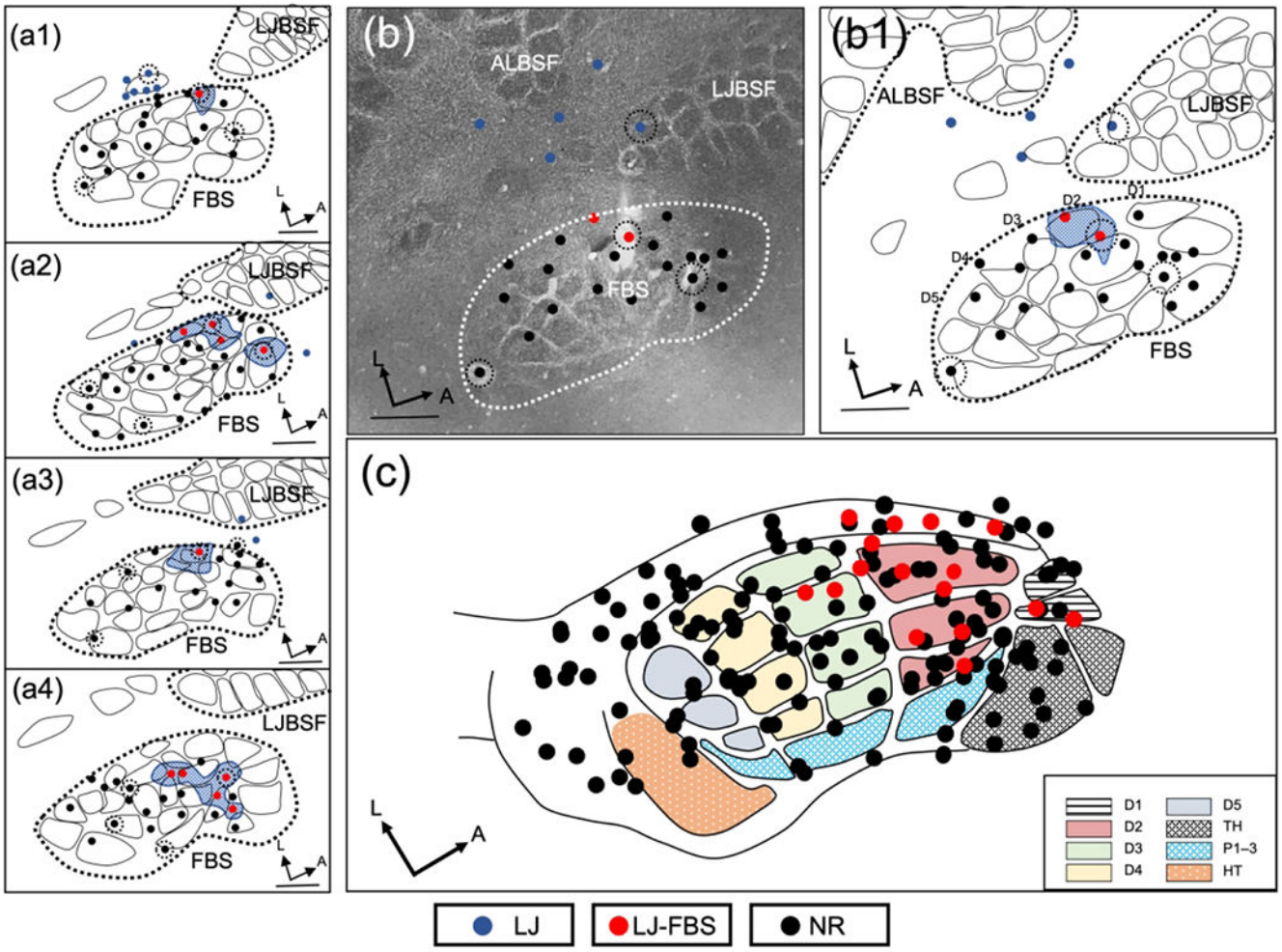

FIGURE 4.

Representation of lower jaw in the deafferented FBS – rapid brachial plexus anesthesia group (rBPA). (a1–a4) Representative examples of reconstructed physiological maps of four rBPA rats, mapped immediately after injection of lidocaine into the area of the brachial plexus. Lower jaw responsive sites in the deafferented FBS (LJ-FBS) are shown with red circles and the areas within the FBS enclosing these penetrations are shown with blue stippling. Lesion sites are designated with black-dashed circular lines around a recording site. Non-responsive recording sites (NR) where lower jaw responses were not found are designated by black circles; lower jaw responsive sites outside the FBS are designated with blue circles. (b) Photomicrograph of CO-stained section and (b1) accompanying line drawing reconstruction showing the location of new lower jaw responsive site in the deafferented FBS. (c) Responsive sites for all data collected in the FBS for seven rats are fitted to the FBS template; lower jaw responsive sites (red circles) and non-responsive sites (black circles). FBS nomenclature shown in box at lower right. Digit one (D1) through D5, thenar pad (TH), digit pads (P1–P3), hypothenar pad (HT), lower jaw (LJ), lower jaw recording sites in FBS (LJ-FBS), no-response (NR). Lower jaw barrel subfield: LJBSF; Anterior Lateral Barrel Subfield: ALBSF. Scale bars = 1 mm.

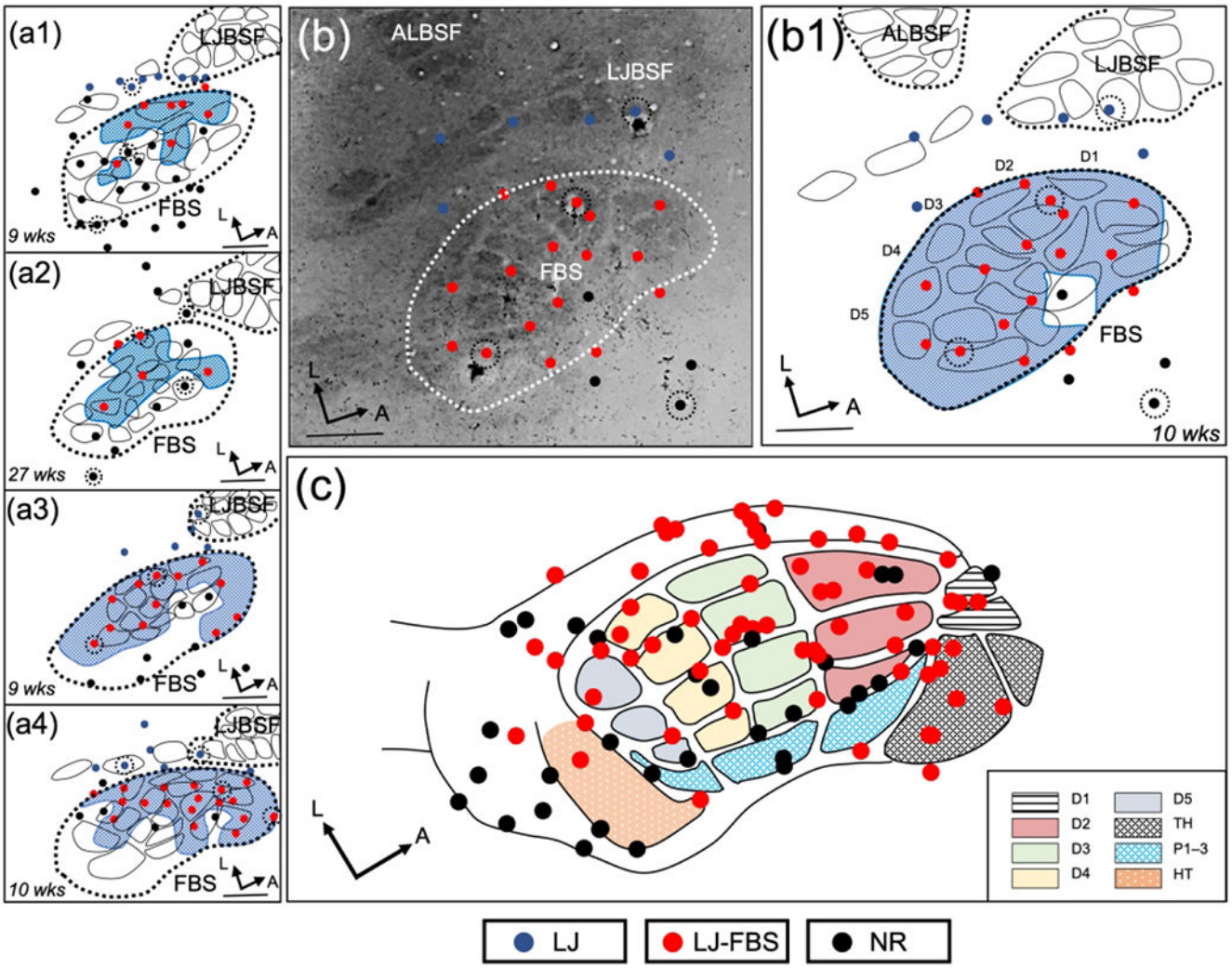

FIGURE 5.

Representation of lower jaw in the deafferented FBS – delayed forelimb amputee group (dAMP). (a1–a4) Representative examples of reconstructed physiological maps from four dAMP rats, mapped 9–27 weeks (wks) after forelimb amputation. Lower jaw responsive sites in the deafferented FBS (LJ-FBS) are shown by red circles and their representational area within the FBS is enclosed with blue stippling. Lesion sites are designated with black dashed circles around a recording site. Non-responsive sites (NR), where lower jaw responses were not found, are indicated by black circles; lower jaw responsive sites outside the FBS where responses were observed after stimulation of the lower jaw are designated with blue circles. (b) Photomicrograph of a CO-stained flattened and tangentially cut section; FBS is enclosed by white dashed line and lower jaw responsive sites are shown with red circles. (b1) Line drawing reconstruction from (b). (c) Composite reconstruction of lower jaw responsive sites from seven dAMP rats plotted on an FBS template. In the dAMP group, lower jaw input is distributed throughout the entire FBS. FBS nomenclature shown in box at lower right. Digit one (D1) through D5, thenar pad (TH), digit pads (P1–P3), hypothenar pad (HT), lower jaw (LJ), lower jaw recording sites in FBS (LJ-FBS),

no-response (NR). Lower jaw barrel subfield: LJBSF; Anterior Lateral Barrel Subfield: ALBSF. Scale bars = 1 mm.

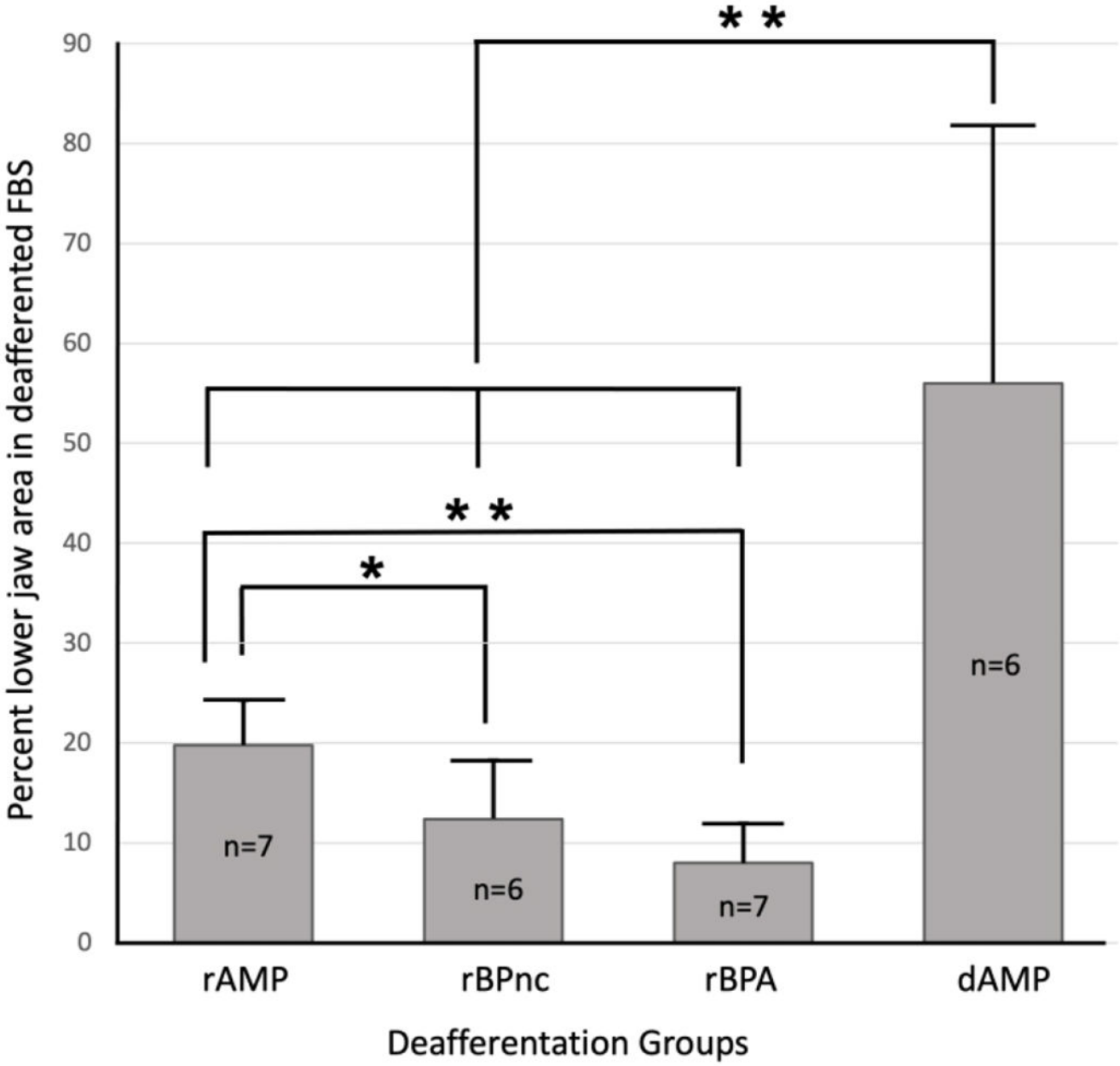

FIGURE 6.

Bar graph showing mean percent lower jaw representation in the deafferented FBS for each deafferentation group. Measurements for mean area comparisons were subjected to the Mann-Whitney U non-parametric statistic with a confidence level of P<0.05* and P<0.01**. rAMP: rapid Amputation Group, rBPnc: rapid Brachial Plexus nerve cut Group, rBPA: rapid Brachial Plexus Anesthesia Group, dAMP: delayed Amputation Group. n: number of rats in each group. Forepaw nomenclature from Fig. 1.

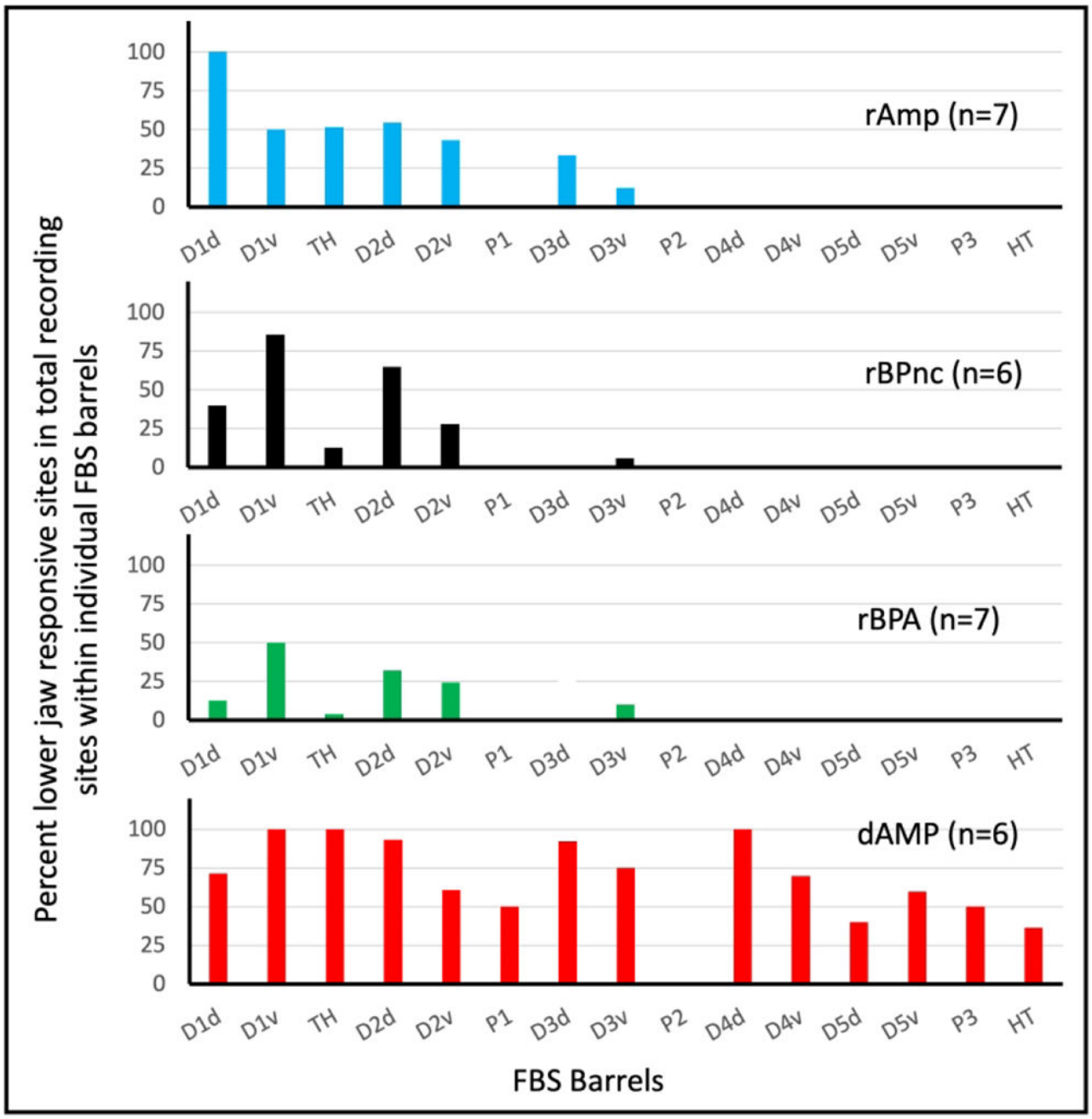

FIGURE 7.

Bar graph showing percent total lower jaw responsive sites recovered in individual barrels and barrel bands in the FBS for each deafferented group. Glabrous ventral digits, D2v–D5v, were organized into digit barrel bands containing individual barrels representing distal, middle, and proximal phalanges of the digit. Even though a ventral barrel band contained multiple barrels, the barrel band was counted as a single barrel unit. rAMP: rapid Amputation Group, rBPnc: rapid Brachial Plexus nerve cut Group, rBPA: rapid Brachial

Plexus Anesthesia Group, dAMP: delayed Amputation Group. n: number of rats in each group.

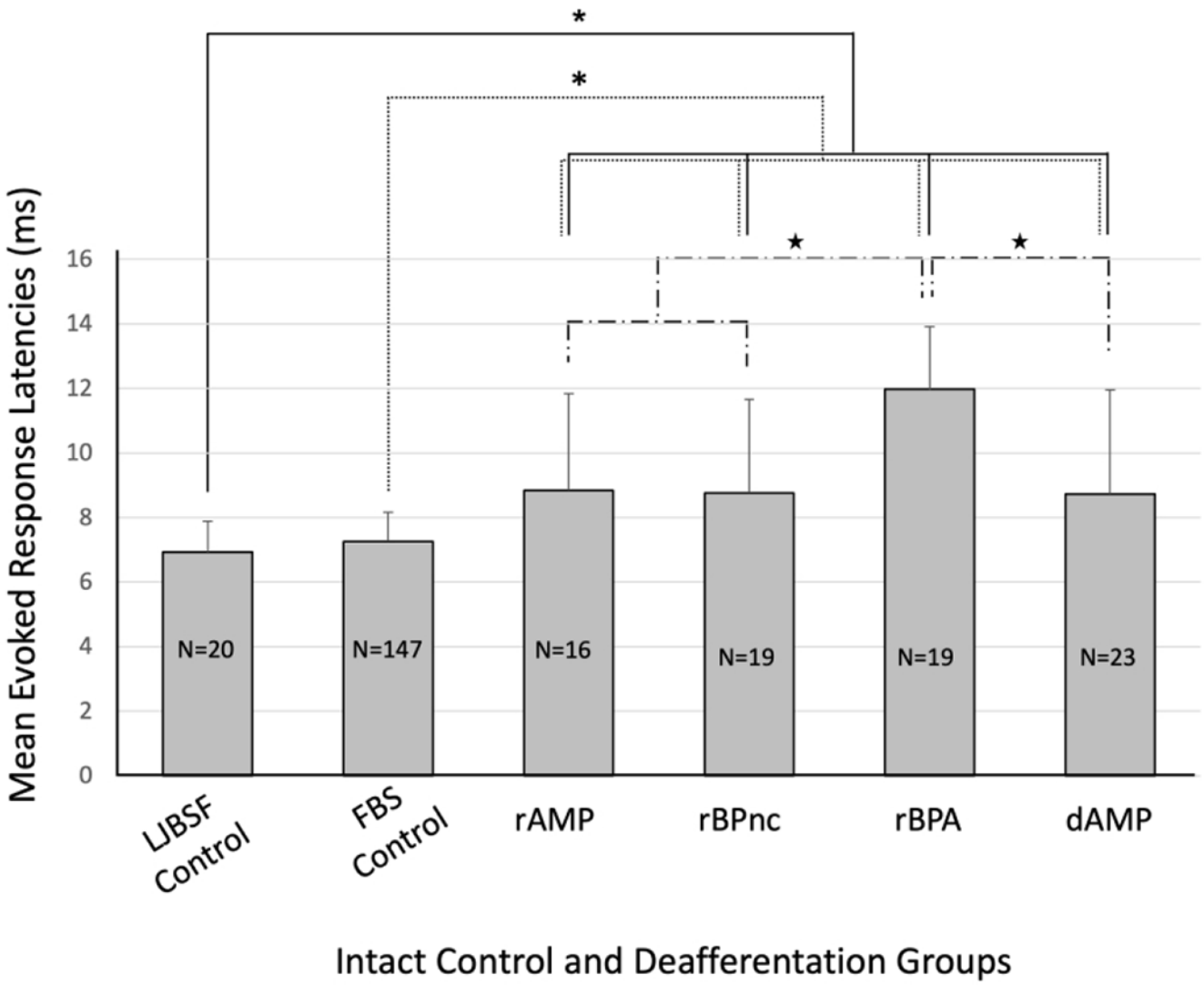

FIGURE 8.

Bar graph showing mean evoked response latencies for forelimb intact and deafferented groups of rats. No significant differences in evoked response latency were observed between control groups, however, control group latencies were significantly shorter compared to each deafferented group. Within deafferentation groups, rBPA evoked response latency was significantly longer compared to the other deafferentation groups. Evoked response latency measurements for intact and deafferented groups were subjected to the Mann-Whitney U non-parametric statistical with a confidence level of $P<0.05$*. rAMP: rapid Amputation Group, rBPnc: rapid Brachial Plexus nerve cut Group, rBPA: rapid Brachial Plexus Anesthesia Group, dAMP: delayed Amputation Group, LJBSF Control: intact lower jaw barrel subfield, FBS Control: intact forepaw barrel subfield. n: number of rats in each group. n: number of evoked response measurements collected in each group.

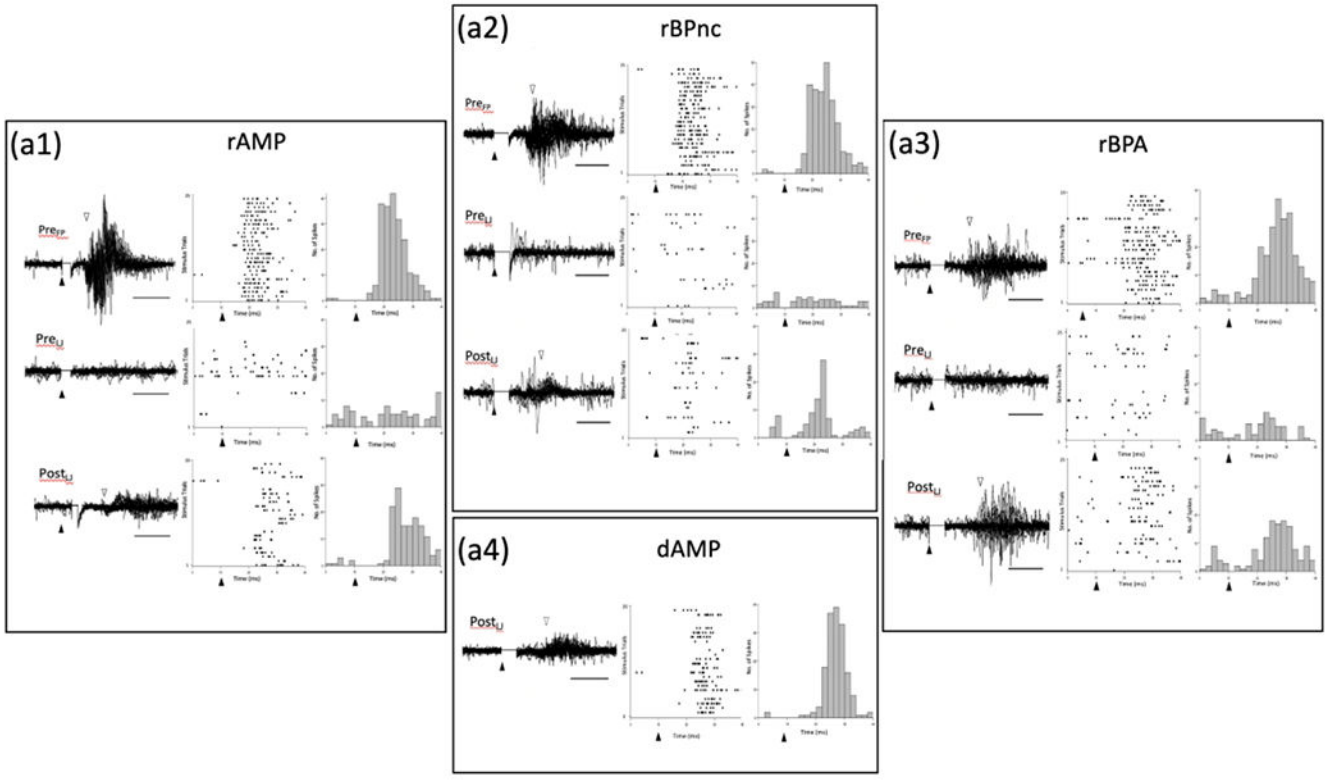

FIGURE 9.

Representative examples of evoked response traces, raster plots, and post stimulus time histograms (PSTH) for each deafferentation group. (a1) rAMP group, Top row – Representative example of evoked response traces recorded in the FBS following 25 consecutive electrical simulations of the forepaw before deafferentation (Pre_{FP}). Solid triangles mark the time of stimulus onset, and open triangles mark the onset of the evoked response. Accompanying raster plots show cell firing for each stimulus trial, and PSTHs show the number spikes recorded in 2 ms bins. Middle row – Representative example of evoked responses recorded in the FBS following 25 consecutive stimulations of the lower jaw before deafferentation (Pre_{LJ}); accompanying raster and PSTH are also shown. Bottom Row – Representative example of evoked responses recorded in the FBS following 25 consecutive stimulations of the lower jaw along with accompanying raster plot and PSTH collected immediately after forelimb amputation. Note the presence of the evoked response following stimulation of the lower jaw which was not present prior to deafferentation. (a2, a3) Representative examples of evoked responses, raster plots and PSTHs for rBPnc and rBPA rats. In each case, lower jaw stimulation evoked a response in the FBS only after forelimb deafferentation. (a4) Representative example of evoked response traces, raster plot and PSTH for delayed forelimb amputee (dAMP) that was recorded 10-wks after amputation. dAMP rats were not tested prior to amputation. Inspection of each rapid deafferented group record shows that the onset of lower jaw evoked responses lagged behind Pre_{FP} recorded latencies. rAMP: rapid Amputation Group, rBPnc: rapid Brachial Plexus nerve cut Group, rBPA: rapid Brachial Plexus Anesthesia Group, dAMP: delayed Amputation Group.

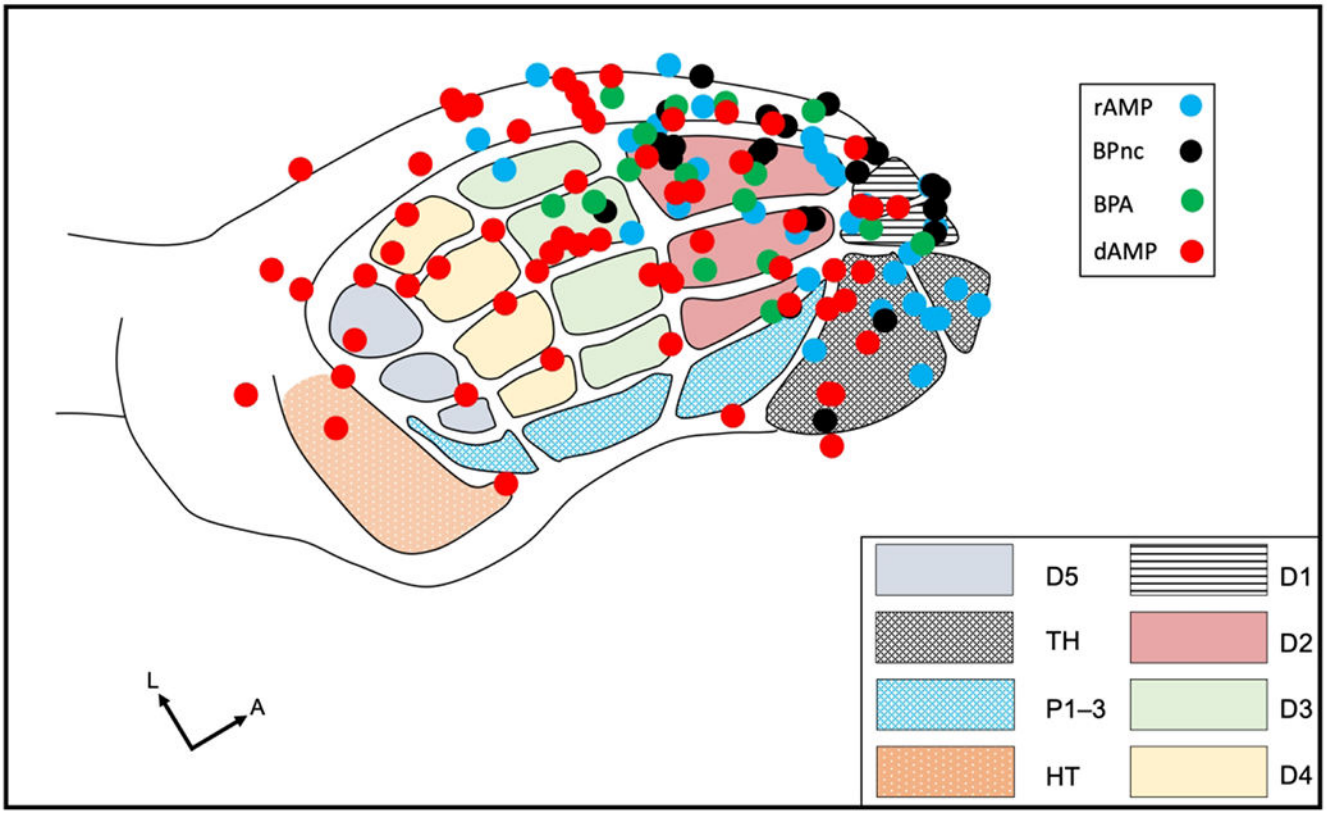

FIGURE 10.

Summary figure showing the sites of new lower jaw responses of each deafferented group plotted on the FBS template. Note the rapid deafferentation group has new lower jaw responses localized in the anterior FBS while the delayed deafferent group has new lower jaw responses distributed throughout both anterior and posterior FBS. rAMP: rapid Amputation Group, rBPnc: rapid Brachial Plexus nerve cut Group, rBPA: rapid Brachial Plexus Anesthesia Group, dAMP: delayed Amputation Group. Digit one (D1) through D5, thenar pad (TH), digit pads (P1–P3), hypothenar pad (HT).

Table 1.

Areal measures of the FBS and lower jaw representation in deafferented FBS for each deafferentation group

Deafferentation Group	FBS Area (mm^2)	Lower Jaw Area (mm^2) in FBS	Percent Lower Jaw Area (mm^2) in FBS
rAMP (n=7)			
Mean	2.95	0.58	19.75
SD	0.25	0.14	4.53
SE	0.09	0.05	1.71
rBPnc (n=6)			
Mean	296	0.36	12.38
SD	0.20	0.16	5.88
SE	0.08	0.07	2.40
rBPA (n=7)			
Mean	3.12	0.25	7.97
SD	017	0.12	4.01
SE	0.07	0.05	1.52
dAMP (n=6)			
Mean	2.91	1 64	55.99
SD	0.16	0.77	25.82
SE	0.06	0.31	10.54

SD: standard deviation

SE: standard error

rAMP: rapid Amputation Group

rBPnc: rapid Brachial Plexus nerve cut Group

rBPA: rapid Brachial Plexus Anesthesia Group

dAMP: delayed Amputation Group